BORICUA SUN

UPRM SOLAR BOAT

Solar Splash Technical Report
May 8, 2017.
Boat #6

Team members:

Alexander Santos
Alan Lopez
Emmanuel Robles
Jose Feliciano
Arnaldo Rivera
Noel Colón
Amanda Santiago
Ignacio Delgado
Diego Capre
Yadiel Marquez

Advisors: Dr. Erick Aponte
Dr. Guillermo Serrano

Executive Summary

The main purpose of the Solar Boat Project at UPRM is to develop an integrated multidisciplinary design applied to solar power electric marine vehicles. Additionally, the Sun Boricua Team was created to enhance the students' educational experience developing their technical and non-technical skills.

After the first participation in the Solar Splash 2016 competition, the team implemented a lessons learned approach to channel this year's efforts. An in-depth analysis of the 2016 results, in comparison to the top 5 teams, paved the path for the 2017 team objectives. The team decided there were fundamental aspects of the design that needed attention and had ample room for further optimization. One of the most significant conclusions was the postposition of the Hydrofoil System Implementation for the 2018 Solar Splash.

The evaluation highlighted the need to design a propeller specifically for the endurance competition and re-design the solar panel along with new battery selection process. For the Sprint competition, the results of the analysis demonstrated the need to re design the power system to reduce the voltage regulation and battery selection process. A new power electronics dc-dc boost converted has been developed, however it requires a new sprint propeller design to achieve maximum performance. Also, weight reduction, characterization of the hull's drag force and improved data acquisition were required.

The following report presents The Sun Boricua Teams Efforts in the areas of Solar Systems, Electrical Systems, Power Electronics Systems, Hull Design, Drive Train and Steering and Data Acquisitions and Communications.

Table of Contents

I. Overall Project Objectives

After participating for the first time in the 2016 Solar Splash Event, Boricua Sun team developed a lessons-learned approach to channel their efforts. The following objectives summarize the team's finding and were the focus of last year's efforts.

- Improve Endurance Performance: Last year the boat performed at 2.1(m/s) for a total of 27 laps with solar panels. The goal this year is to achieve 2.6(m/s), without solar panels, for a minimum of 33 laps. Strategies include: accurate drag measurements, optimized endurance propeller design, and revision of battery selection process.
- Increase Solar Panel Capacity: The original solar panel array supplied 460W of power.460(W). The goal this year is to implement a custom made 530W solar panel. Implement a 530(W) Solar Panel made in house.
- Improve Sprint Performance: The team's best performance in the 2016 competition was 53 seconds. This year's goal is to achieve less than 30 seconds. Strategies include: drivetrain re-design, power system re-design, dc-dc boost converter along with a new sprint propeller and battery selection evaluation.
- Weight Reduction: The goal this year is to achieve a 20% weight reduction.
- Improve Data Acquisition: This is critical aspect because it enables design validation and testing.

II. Solar System

A. Solar Panels

1) Current Design: This sub-team had the task to design and build a custom solar panel that could outperform our previous commercially built solar panels. The previous array was composed of two HighFlex Solar-HF234 solar panels, which could produce 234 Watts each, totaling at 468 watts. Although lightweight (6.6 lb.) and reasonably efficient (19.2% at STC), they were not producing the maximum power output allowed by the Solar Splash competition, which is 528 Watts for student-built arrays. Restricting PV array power and dimensions to what is commercially available could mean a significant difference in performance for the boat.

2) Analysis of Design Concepts**:** To manufacture the PV array, we had to obtain solar cells that met our design requirements as closely as possible. The SunPower Maxeon solar cells were a good match. These cells are ~22.5% efficient, 125 mm^2, semi flexible monocrystalline silicon cells. Each cell produces 3.45 Watts @MPPT. To achieve power production as close as 528 Watts, 153 cells are needed, producing a maximum of 527.85 Watts. This new configuration with more power would increase the dimensions of the panel's structure compared to last year's. The configuration chosen was divided in 4 separate arrays as depicted in Fig. 1. In solar panels, relatively small shades can cause major negative impact, as far as eliminating most of the current produced on arrays in series. The main electrical goal was to get the most panels in parallel that could meet our minimum voltage required to charge a 24V battery bank.

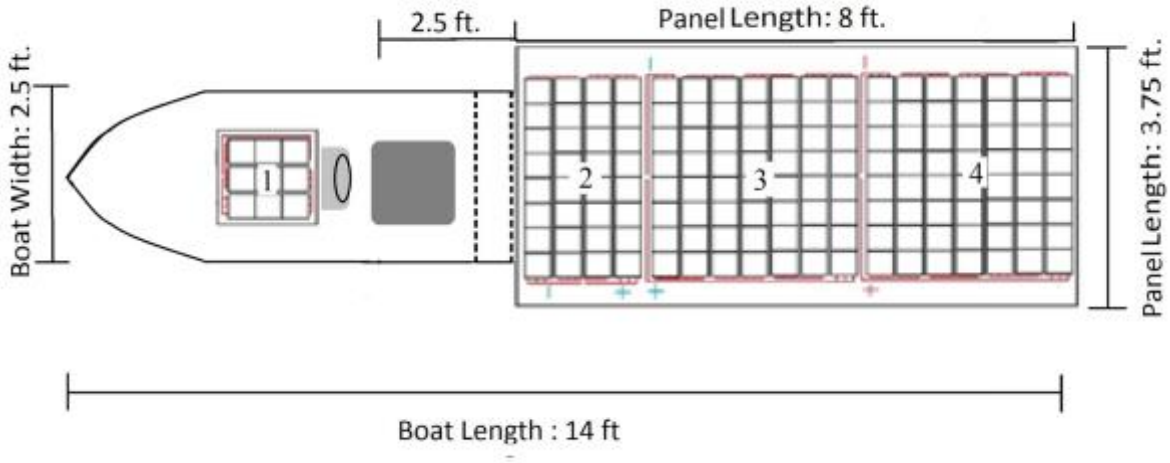

Figure 1: Conceptual diagram of solar panel's assembly with respect to the boat.

Panel 1 has 9 cells in series. Panel 2 has 32 cells in series. These two panels are the closest to the driver, therefore they are most susceptible to receiving shade. Between these two in series, they represent less than ⅓ of our total power produced so, in any case, it makes sense to lose these array's power instead losing the bigger arrays (3 and 4).

Regarding the solar panel fabrication, two prototypes were initially considered: a semi flexible like last year's array, and a solid, lightweight model. After construction, we determined that it

was best to develop a rigid, lightweight solar panel due to lack of machinery needed to make a flexible solar panel. The chosen PV consists of 5 layers: front sheet, front encapsulation, solar cells, back sheet and a strong foam as base, as shown in Fig. 2. Encapsulation was chosen in this manner to protect the cells and to provide adherence to the front and back sheet.

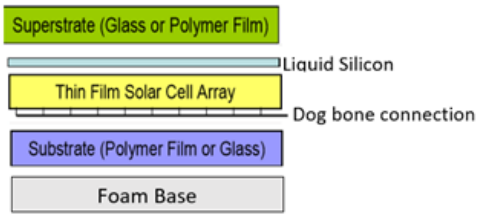

Figure 2: Cross section of proposed solar panel assembly.

For the top, a clear polycarbonate Lexan sheet was chosen instead of glass since it can provide rigidity without adding much weight. For the encapsulation, En-Sil Solar Encapsulation Silicon was used. During the construction of the initial prototypes, although pricier, a clear liquid silicon was easier to apply compared to EVA, since it did not require a heating and molding phase. For the back sheet, any strong, thin polymer could have been used. A white TPT film from Gehring Corp., usually used for solar panel backing was chosen due to its strength, flexibility and because it is relatively lightweight. Instead of using a heavy fiberglass and aluminum base as used last year, a Foamular 250 insulation foam sheet of 2 inch of depth was used. The entire foam base weighs only 10.5 lbs.

Last year's BlueSky Energy 1524ix charge controllers are still favorable for this year's solar panel configuration. The 1524ix is a step-down solar charge controller with Maximum Power Point Tracking (MPPT) technology. Each charge controller can handle up to 400 watts for a battery bank of 24V with an optimal panel voltage range of 33V-37V. An electrical circuit diagram of the solar system is shown in Fig. 3. Panels 3 and 4 are connected directly to the charge controller delivering a current of 11.86A. An additional boost stage is now required for the panels 1 and 2 (refer to Fig. 1) as their ~23V output voltage will fall short for the 33V required by the converter.

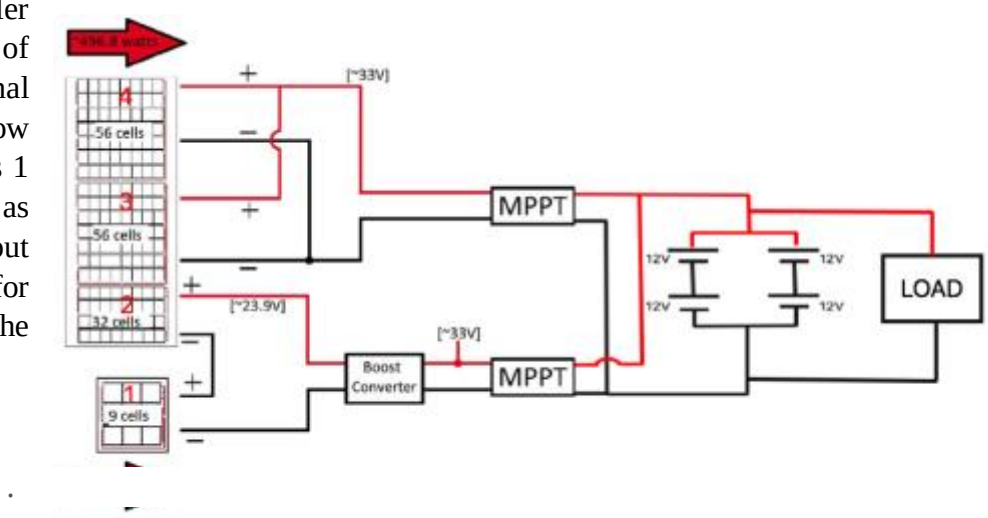

Figure 3: : Electrical circuit diagram of the solar system implementation

3) Design Testing and Evaluation: Table 1 shows a summary of the electrical and physical characteristics of 2016 and 2017 solar panel array. Preliminary testing of each solar panel resulted in a short circuit current of 6.27A and open circuit voltages of 37V and 6.1V for panels 2-4 and 1, respectively (refer to Fig. 1). At this early testing stage, real world graphs for the points of operation at different solar irradiations have not been done, but will be completed by the competition.

Table 1:Solar panel electrical and physical characteristics.

Parameters	2016 Array	2017 Array		
# Panels	2	2	1	1
Dimensions	59”x39”x0.07”	395”x45.25”x2”	395”x45.25”x2”	16.5”x16.5”x2”
Configuration	54 cells/series	56 cells/series	32 cells/series	9 cells/series
V_{mppt} (V)	27.8	32.59	18.62	5.24
I_{mppt} (A)	8.43	11.86	5.93	
Watts	468	527		
Cell efficiency	19.5%	22.5%		
Total Weight (lb)	42.3	28.2		

B. Battery Bank

1) Current Design: Last year’s electric system design used two Duracell SLI24 connected in series for both the endurance and sprint part of the race. This represented a loss of 12.8V at 350A. This year Odyssey Extreme Series batteries were utilized.

Table 2:Sprint and endurance battery configuration relevant specifications

Event	Year	Battery	Config.	Eq. Series Resistance	Voltage	CCA / Capacity
Sprint	2016	SLI24	2 – series	24.2mΩ	24 V	550 A
	2017	PC1100 PC 950	[2 PC1100 – series] series [2 PC950 – parallel]	13.5mΩ	36V	500 A
Endurance	2016	SLI24	2 – series	-	24V	45 AHr
	2017	PC1100 PC 950	[2 PC1100 – series] parallel [2 PC950 – series]	-	24V	60 AHr

2) Analysis of Design Concepts: Battery configuration for sprint segment of the race consisted of two Odyssey Extreme PC1100 in series with two Odyssey Extreme PC950 in parallel. This configuration was selected based on the maximum voltage and the cold cranking Amperes supplied by the configuration. This design will increase Cold Cranking Amperes from 550A to 900A and the voltage from 24V to 36V. The endurance configuration consisted of two Odyssey Extreme PC1100 in parallel with two Odyssey Extreme PC950. Since the maximum weight from the batteries allowed in the competition is 100lbs this configuration provides the most capacity while still staying under the weight limit. A configuration of two PC1100 in parallel with two PC1100 was considered, but that configuration exceeded the maximum weight limit for the competition by 10lbs, the better alternative10lbs therefore, a combination of PC1100 and PC950 in parallel was implemented Table 2 presents a summary of battery bank specifications for the endurance and sprint event compared to 2016 configuration.

3) Design Testing and Evaluation: The BK 8500 DC load and the PV8500 software were used to obtain battery discharge profiles. Batteries were discharged individually at 10A, 15A, and 20A (refer to Fig. 4). Then, two PC950 and two PC1100 and a combination of one PC1100 with one PC950 in parallel configurations were discharged. Graph #1 shows comparative results of batteries discharged at 20A. The PC950 were discharged in 148 mins, the Duracell SL24 were discharged in 158, the PC1100 were discharged in 196 mins. Using the data from battery discharges and some parameters given by the manufacturer the Peukert coefficient (refer to table 3) was calculated for the discharge model. With that model, it was possible to predict the time it would take a battery to discharge at 15A based of the time it would take to discharge the battery at other rates. Fig. 5 shows the accuracy of such model.

Table 3:Comparative Data for Sprint Race

Battery	#Peukert$_E$	#Peukert$_M$	2Hr Discharge Current
Duracell SLI24	1.1286	1.1286	28.81
Odyssey PC1100||950	1.10265	1.1797	30.75 A

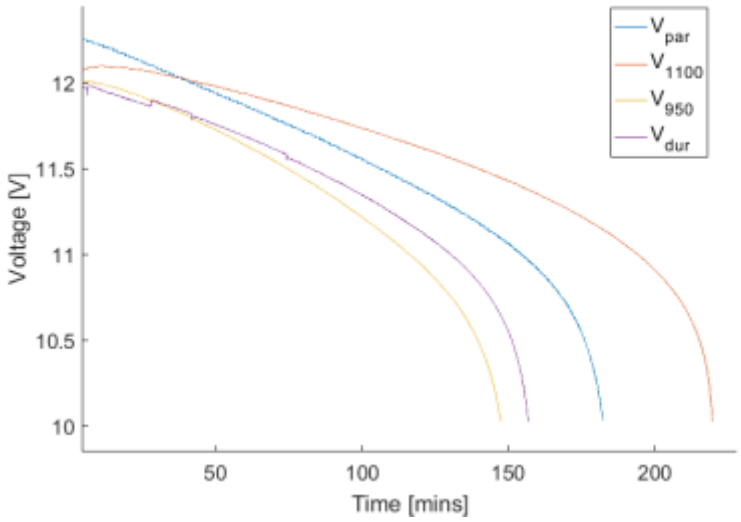

Figure 4: Discharge Rate Duracell vs. Odyssey Extreme PC1100 & PC950 in parallel

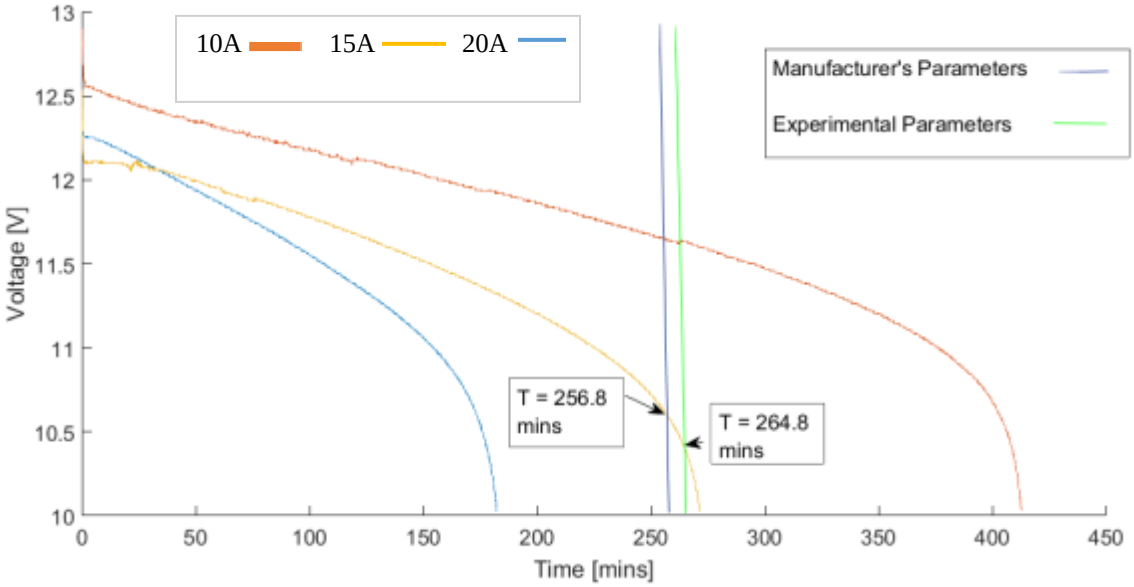

Figure 5: Battery Model Validation

III. Electrical System

A. Efficiency Optimization

1) Current Design: The previous electrical system was identified to have some deficiencies. To have an improved performing solar boat, these deficiencies must be taken care of. Last year's team used an electrical system powered by two Duracell SLI24 batteries because there was no data recollection during the Solar Splash. The analysis was made based on the tests conducted in December 2016 with 36 V batteries and extrapolated to 24 V to calculate, as realistic as possible, the performance's improvement of this year's electrical system, in comparison with the one used for last year's competition. After recollecting data from sprint tests, the team identified that the two biggest offenders for the boat's overall efficiency were battery inner resistance and parasitic resistance. When using 36V batteries for sprint tests, the average voltage drop due to inner battery resistance was 7.63V using Duracell SLI24 batteries. Also, a 5.59V voltage drop was credited to the cable's resistance throughout the boat's electrical system. On average, the inner battery's resistance was calculated experimentally to be 36.3mΩ while the parasitic resistance resulted in 26.5mΩ. Even though these resistance values are relatively small, because the batteries supply an average of 200A, the voltages drop in the electrical system at high currents were very significant, ranging from 12V to 15V.

2) Analysis of Design and Concepts: Considering that the inner battery's resistance was a main contributor to the voltage drop across the electrical system, it was decided to research which battery was better suited for the electrical system. Hence, the Duracell SLI24 batteries were replaced with the Odyssey Extreme PC1100 and PC950. When performing the characterization of the new batteries, it was evident, from a previous 36.3mΩ inner battery resistance, the new battery only presented a 13.86mΩ, when connecting in parallel a PC1100 and a PC950. At high currents, like those typically found in our electrical system for sprint, the new batteries would present approximately a third of the voltage drop in comparison to the previous configuration. On the other hand, to further improve efficiency, a complete electrical system reconfiguration was made, considering that the previous system presented high parasitic series resistance. The two main objectives were to reduce cable length by optimizing space and to increase the cable's cross-sectional area by changing from AWG (1 /0) to ¼" x 1" copper bus bars. Because resistance is proportional to cable length and inversely proportional to the cable's cross-sectional area, by reducing our conduction resistance it would translate, at high currents, on a reduction in voltage drop.

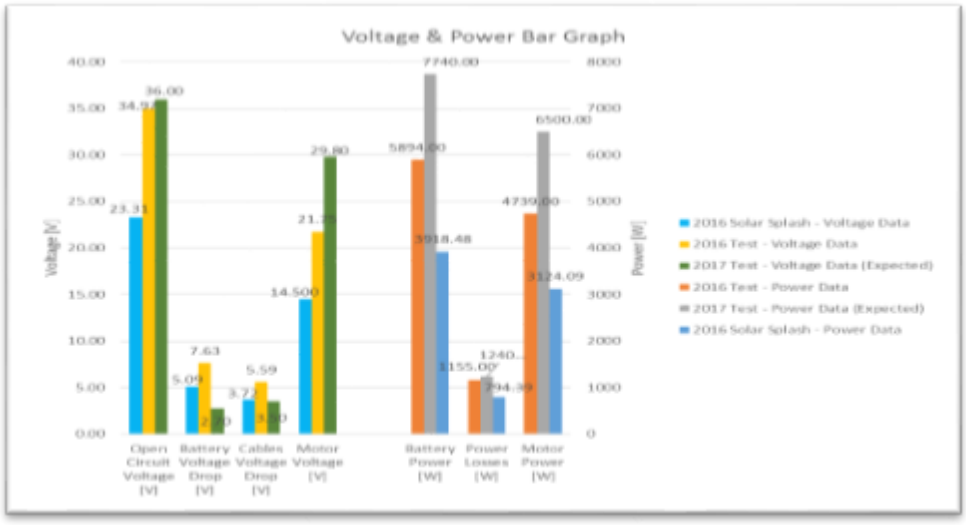

Fig. 6 *Comparative Bar Graph between previous and new Electrical*

3) Design Testing and Evaluation: The implementation of copper bus bars helped reduce the parasitic resistance, including the unnecessary switches, connections and the weight found in boxes and materials. In addition to the benefits previously mentioned, it helped reducing space occupied by the electrical system, which is demonstrated in Fig. 8. It is with the assistance of sensors that this data is stored providing the possibility to analyze the data and reach conclusions about improvements. Referring to the Fig.7, showing the comparison between recently measurements and simulations of the Solar Splash 2016 performance we can see how the performance in sprint has improved greatly, which is a way to test the decrease in voltage drop at high currents, improving time in the 300 meters and increasing the average speed. It can also be used to validate newly integrated components. When analyzing the electrical system performance, the variables that are being stored and used are battery voltage, battery current, motor voltage, motor current, and RPM. For the construction of the bar graph shown in Fig. 6, we used experimental data from December 2016 and March 2017. To identify this year's improvement in efficiency and performance, the experimental data of December 2016 was extrapolated to represent that of last year's Solar Splash.

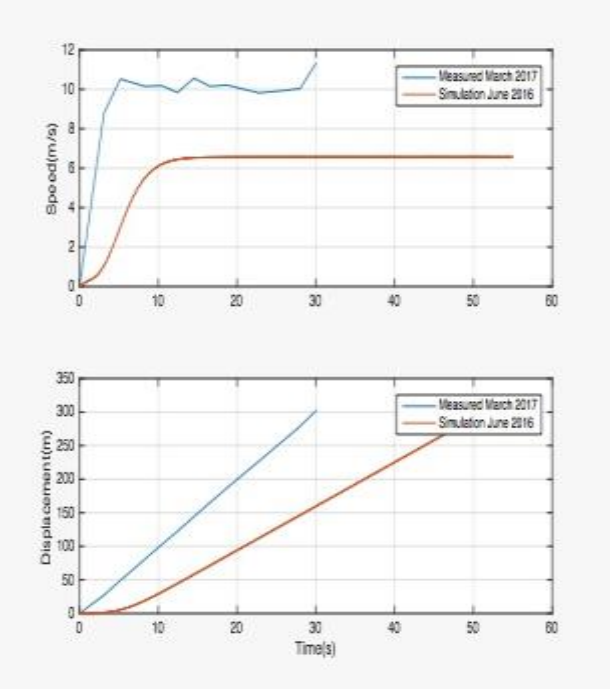

Fig. *7 Speed and Displacement comparison*

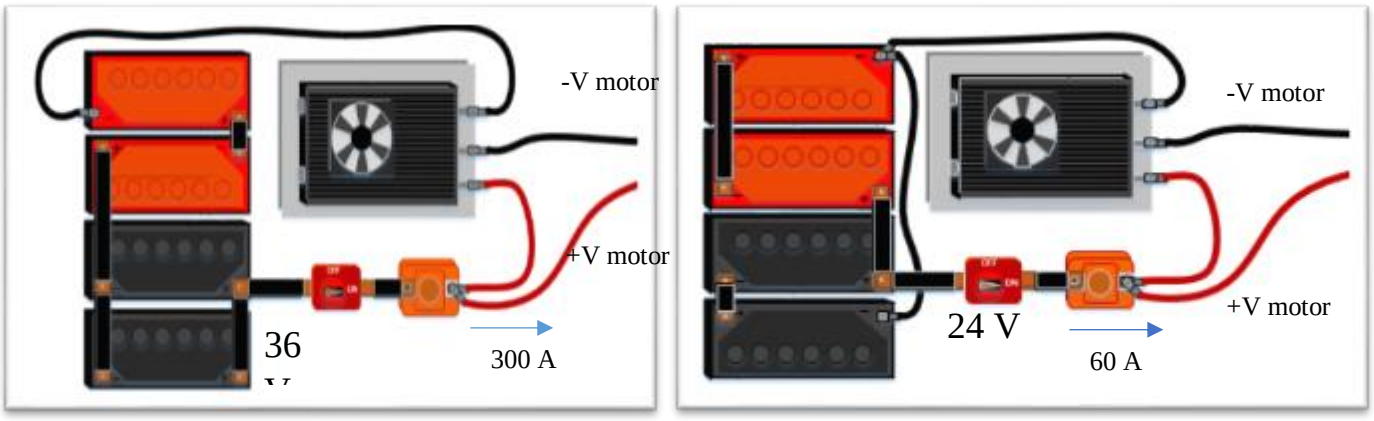

Fig. 8 Latest Sprint and endurance configurations with copper bus bars

B. Discharge Analog Controller

1) Current Design:

Last year design had no automatic system for constant discharge of the batteries. The boat driver would use a voltmeter and maintain a constant velocity that would discharge the battery at an average rate that was close to what was desired.

2) Analysis of Design and Concepts:

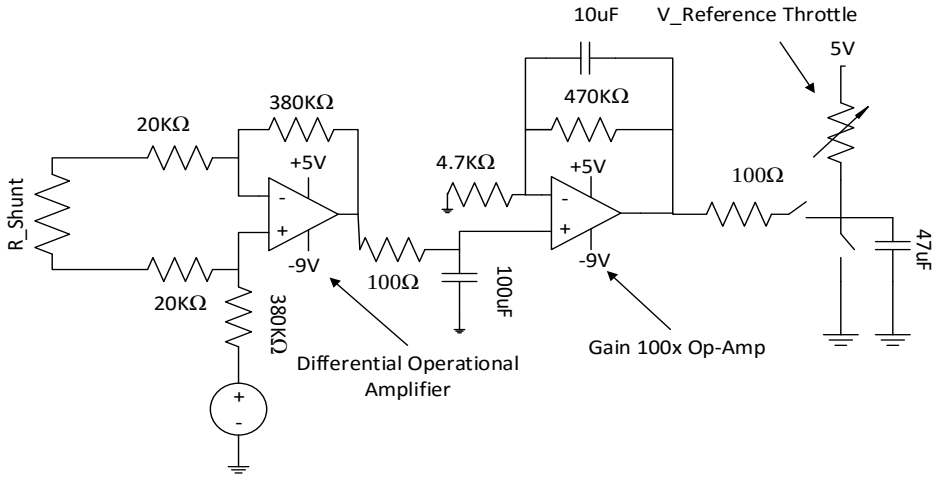

Figure 9: Schematic for discharge analog controller

Using the mathematical model and the parameters obtained through the battery discharge profiles, optimal discharge rate of the battery bank was identified as 30A. This discharge rate is of interest due to the endurance competition. As shown in Fig. 10 the solar panels are connected in parallel to the motor controller and the battery bank, because of this if the boat maintains constant speed, the variations in current supplied by the solar panels will cause the same variation in the current supplied by the batteries. To achieve maximize performance constant current is needed. A circuit that will change the duty cycle of the controller if the

current from the batteries changes from 30A was implemented. The circuit consist of one differential operational amplifier AD629ANZ and a non-inverting operational amplifier with a gain of 100 (refer to Fig. 9). The AD629ANZ will compare the voltage drop in the shunt resistor and compare it with a reference voltage, if the voltage in the shunt is below the reference voltage the output voltage will be positive, the second stage will amplify the output to raise the duty cycle and therefore increasing the speed of the motor. A higher speed will require a higher current passing through the shunt resistor and once the current passing through the shunt reaches 30A the output will become 0V. The circuit also has some capacitors to filter noise and to keep it stable.

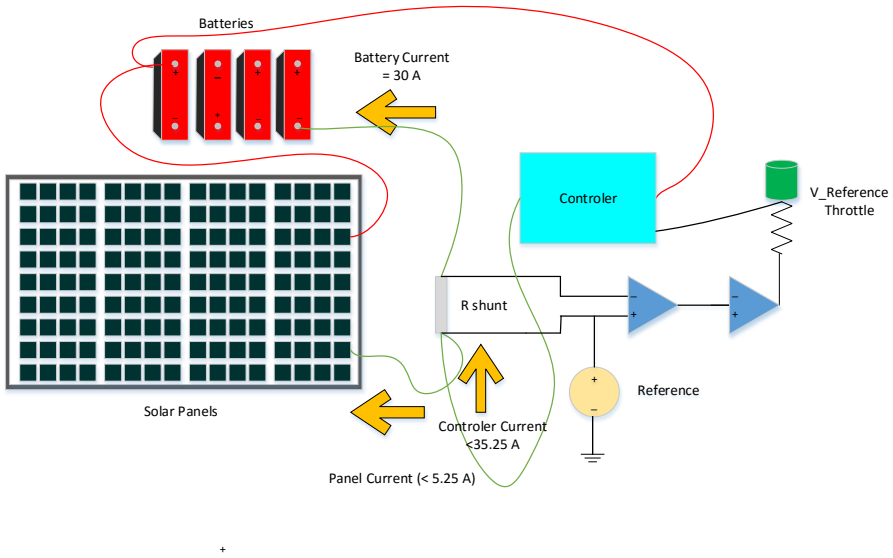

Figure 10: Discharge Analog Controller Implementation

3) Design Testing and Evaluation

At this moment, the circuit has not been implemented therefore the evaluation of the system has not been able to be completed at this point.

IV. Power Electronics System

A. DC/DC Boost Converter

1) Current Design: Super capacitor System, currently a step-down Chopper converter (Kelly controls KDH12601e) is implemented, but it can only have a maximum output voltage of 36 volts. To try to achieve the 52 volts of output voltage, the previous implementation tried to connect a super capacitor that charged in parallel with the batteries and discharged in series with the batteries. The system with the super capacitor can never be achieved properly for several reasons. We will discuss only the two most important. The first reason is that they need too many connections and switches, and this creates a voltage drop of 10 volts. These power losses created an inefficient system for the solar boat in the competition.

2) Analysis of Design Concepts: Competition rules limit to 36 volts the voltage in the batteries and no more than 52V at any point in the boat. For this reason, we wanted to eliminate the super capacitor and design a new DC / DC boost converter of 36 volts input and a maximum output voltage of 52 volts to add a new stage (refer to Fig. 11) to deliver 52 Volts to the chopper converter. An important specification taken into consideration was that there could be no more than 400 Amperes at the converter output, because this is the maximum current that the motor can handle for one minute. The boat has an Agni 95 DC motor able to operate at a maximum of 72V. The input current of the DC/DC converter is limited by the batteries that have a maximum current of discharge of 600 amps for one minute. With this improvement, the motor will give more power to the propeller and a higher efficiency with 52 volts rather than 36 volts.

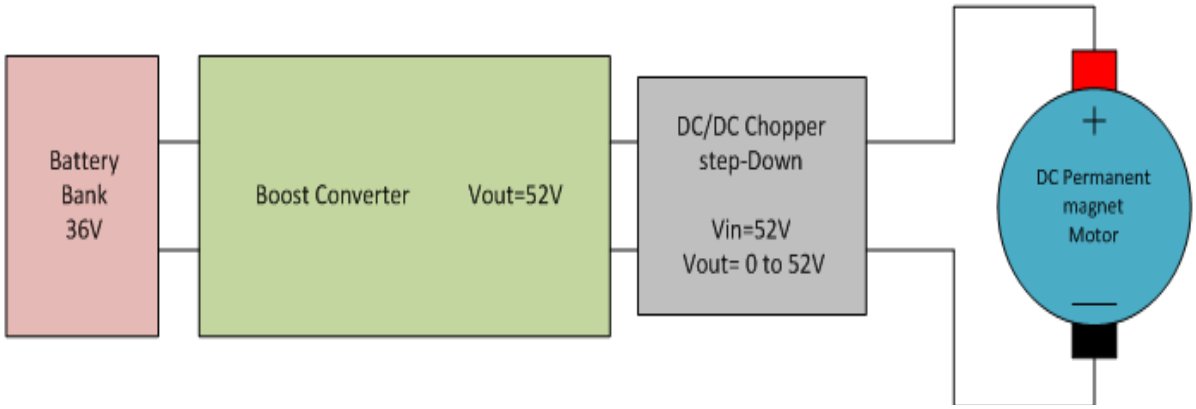

Figure 11: Power sprint configuration

Using this boost converter, the motor will have a new point of operation. Therefore, at 52V, using the last propeller, the current required to operate the motor is more than 400 amperes, and this can cause damage to the motor. This problem is illustrated in Fig. 12. It was necessary to design a new propeller for sprint to match a new point of operation in the motor with a current less than 400 amperes when the voltage in the motor is 52 volts.

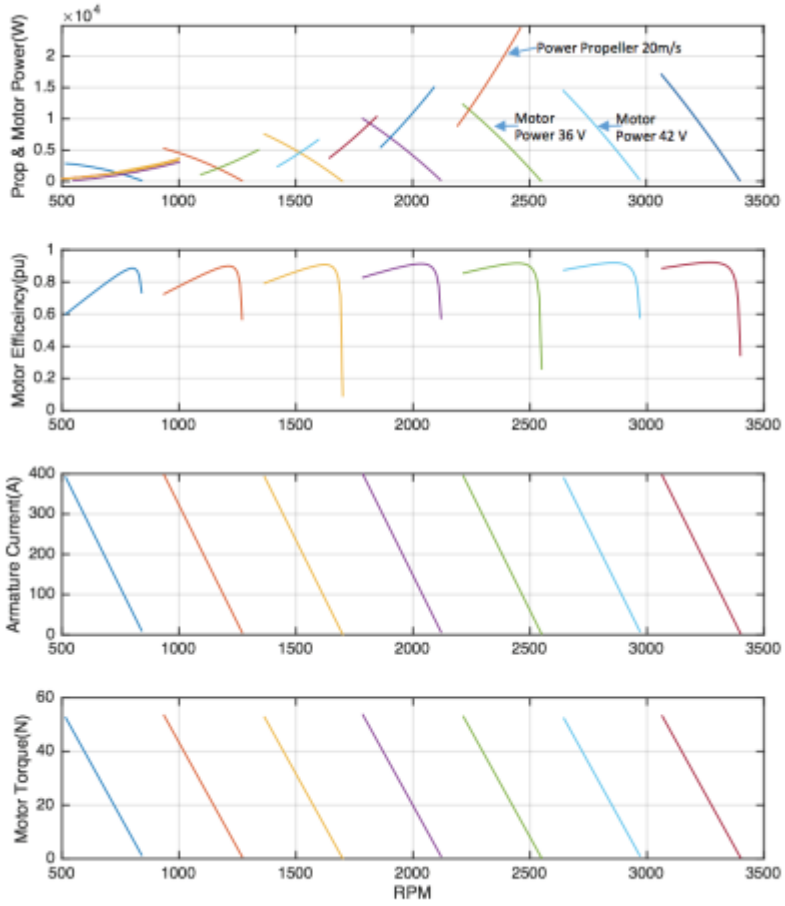

Figure 12: Motor points of operation and propeller

3) Design testing and Evaluation: DC/DC Boost Converter Control System- As part of a Boost Converter, is necessary to design a control system circuit. This circuit need to be able to control a Transistor with a PMW signal with a duty cycle that change. This change in the duty cycle is determinate or proportional to a measure or signal in the circuit. For this project, the feedback or signal of the circuit used for determinate the value of de duty cycle is the output voltage. Also, the input current is measured for turn of the circuit in case of over current. This circuit has a driver circuit that is isolated from the microprocessor or control circuit. The purpose of that isolation or optocoupler is to reduce the effect of noise or distortions in the control system or microprocessor.

Fig 13 represents the circuit implemented to control the boost converter. The area in the schematic named as "CONTROL_CIRCUIT" has an Arduino Leonardo to process the feedback signals and generate the PMW for the driver. Also, this part has two voltage regulators, one of 8 volts for the microcontroller and one of 5V for the circuits "BOOST_VOUT" and "BOOST_CURRENT. The "BOOST_VOUT" and the "BOOST_CURRENT" are two circuits that has differential amplifier (AD629ANZ) with a

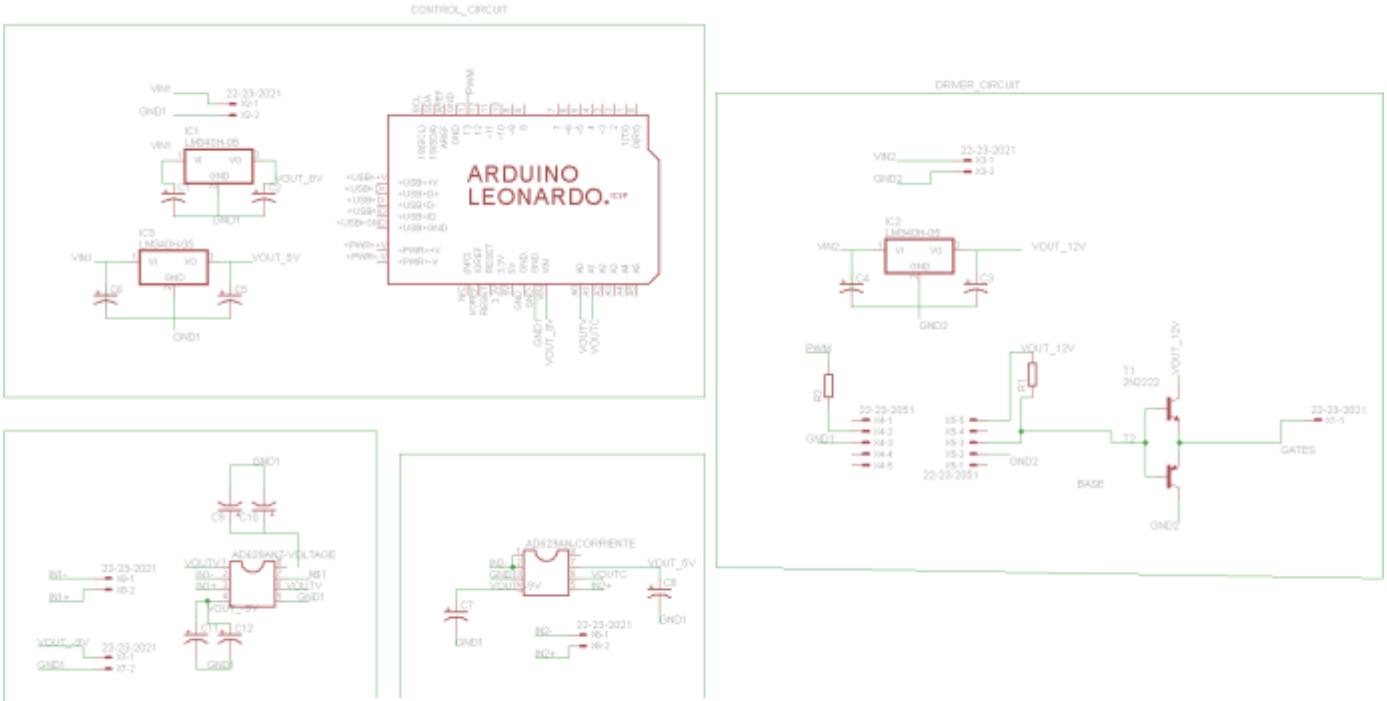

Figure 13: Control system schematic

different configuration with the purpose to have a different gain of amplification. The "BOOST_VOUT" circuit has a gain of 1/19 and the "BOOST_CURRENT" has a gain of 19. The "BOOST_CURRENT" circuit measure a voltage drop of a "SHUNT" resistor. This voltage has a representation in the current that past across this resistor. The "DRIVER_CIRCUIT" is the circuit that isolate the boost converter to the microprocessor. Also, this circuit amplified the PWM signal produced for the microprocessor. This circuit has a different ground.

Boost Converter Copper Plate Circuit Fabrication- The testing of design the DC/DC converter is still being made. The analysis conducted for calculate and selection the sizes of the conductors for the boost converter, the heat sink and thermal management calculation and boost converter design are in the appendix F.

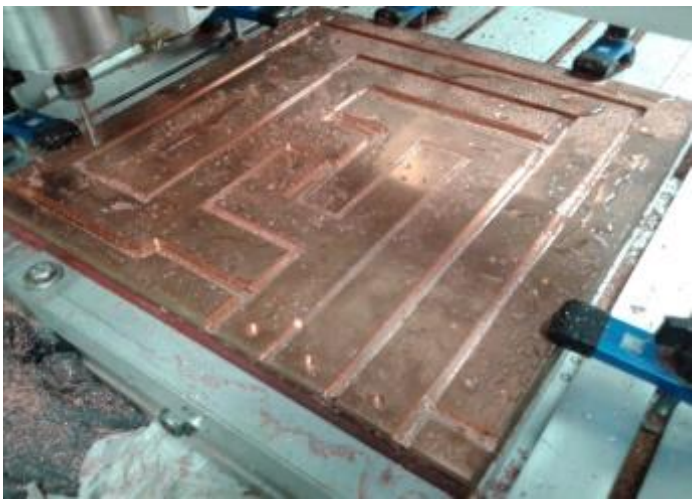

Figure 14: CNC Machine Copper Cutting

Testing for the DC/DC converter design (see Fig. 14) is still being made. The analysis conducted to calculate and select the sizes of the conductors for the boost converter, heat sink, thermal management calculation and boost converter design are in the appendix F.

V. Hull Design

A. Current Design: Last year, the Boricua Sun team tried to implement a variable angle of attack hydro foil system. The main problem was the complexity of the hydrofoils control system. This problem produced a change on the plan and the team decided to temporarily discard the hydro foil system. The design is still relevant and we might revisit this approach in the future.

B. Analysis of Design Concepts: The simplification of the system meant that the hull should be characterized with regards to the hull drag, to further analyze the performance. The approached method consisted of tying up the boat and pulling in favor a against the current, while measuring speed.

C. Design Testing and Evaluation: Afterwards, the results from both test were averaged to obtained a polynomial describing the hull's drag with respect to the ship speed. Fig. 15 contains the representation of the 2 curves that describe the test results and the curve that describes the average behavior of both tests. The resulted polynomial ($14.573V^2+19.919V+6.385$) was implemented in the analysis and development of the endurance propeller.

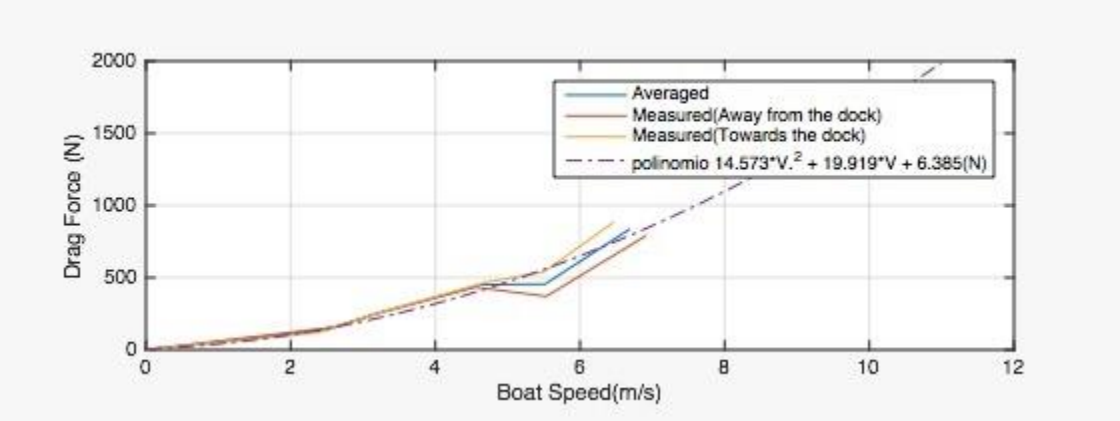

Figure15: Drag Force versus Boat Speed

VI. Drive Train and Steering

A. Drive Train

1) Current Design: The previous design (refer to Fig. 16) was composed by a long drive train that held a transmission for hydrofoils with variable angle. The connection between the transmission with the propeller and the DC motor is the stainless steel shaft that goes inside the drive train. The transmission is a Yamato 302 with a gear ratio of 1:0.93. A coupling was connected to the shaft and the Yamato transmission and we connected another coupling between the motor and the shaft. There are two aluminum plates that connects the motor case and the transmission.

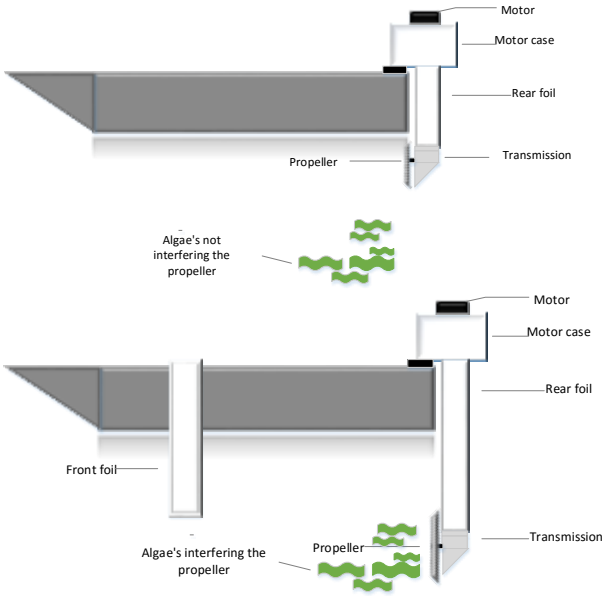

Figure 16: Current and New Drive Train System Diagram

Last year, the main problem was the complexity of hydrofoil control system. Hydrofoils remain a relevant technological breakthrough. However, due to time constraints the team decided to postpone the hydro foil systems.

Last year during the competition, the team spotted several issues. The original drivetrain was long and had problems with shallow waters and tangled algae in the propeller, this created an inefficiency on the system. In addition, another problem found was that the propeller performance was inefficient for the endurance competition and this was due to the fact that the propeller was designed for higher velocities.

In order to improve competitiveness, the team decided to manufacture a drivetrain system that could be effective in an outboard boat. The system needed a different position for a better performance during the sprint and endurance competition. This implies a shorter shaft and a new connection to the transmission that received a reduction on drag force to transmit a higher efficiency on the velocity. The goal was to create a drivetrain system reliable and efficient.

2) Analysis of Design Concepts: The new drive train system (refer to Fig. 17) for the boat applies the concept of a standard outboard boat. The main goal is to create a drive train system with individual specs for each event of the challenge. In the designing process of the new drive train system the team took in consideration some important factors for optimization such as efficiency, speed and reliability. To connect the motor case and the transmission, the team decided to create a mid-section foil form to reduce the drag. To transmit the motor power to the transmission the team use a shaft. The material of the shaft is a 316 stainless steel with a yield point of 30ksi and the ultimate tensile strength of

75ksi material properties on appendix. It is unacceptable for it to fail by stresses or fatigue cycles. To prevent a failure on the shaft, the team analyzed the shaft deformations and the safety factors. For structural analysis the formulas of DET for Von Misses maximum stress was used and for dynamic test the theory of Modified Goodman. The only stress affecting on the shaft is torsional. With the fig.G1 the tam used it to calculate the power that is providing the DC motor to the shaft. The static analysis gave us a safety factor of 1.11 and the dynamic analysis gave us a safety factor of 2.85. All the calculations of safety factor can be obtained on the appendix. The shaft was directly connected to a Jaw coupling hub, this coupling was donated by a company called Roland manufacturing, coupling specs on appendix. The transmission was carefully aligned using two aluminum transition plates with a silicon sealer to ensure that there is no fluids exchange, these plates also act like the transition and adapter of the transmission to the aluminum foil built. All the manufacturing process was elaborated with a lathe, milling press machine and CNC.

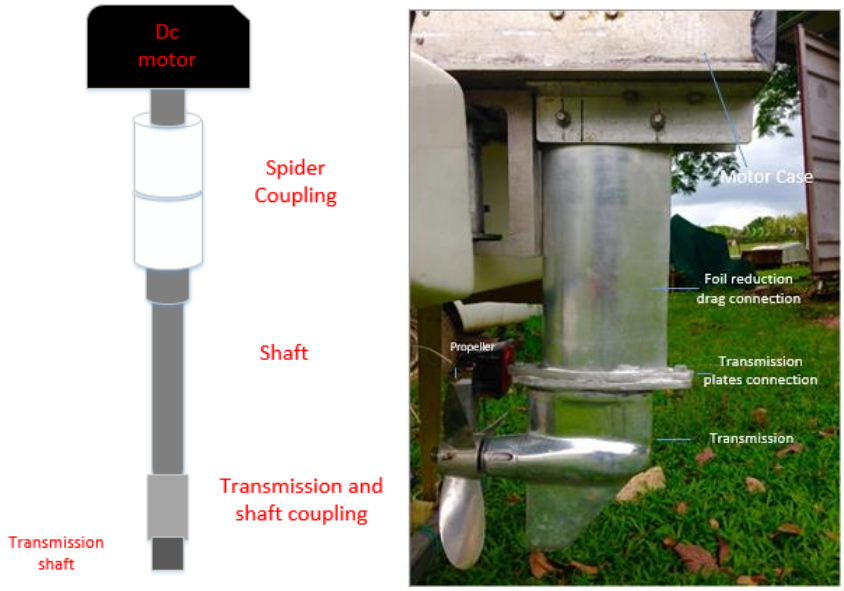

Figure 17: New drive Train system assembled and inner drive train system diagram

3) Design Testing and Evaluation: The team was able to test it early this year. During the test, the team was able to view the performance for the sprint drive train assembly and get a significant change on the speed. Last year, using the instrumentation the highest velocity recorded was 6 m/s; with the new system, the boat reached a velocity of 11.44 m/s. On figure 18, we can see the difference between tests during this year. This increase on the velocity represents 89.62% higher, compared with the previous drive train system. The problem about striking topographical features was fixed because the propeller was in a higher position and the sedimentation amongst algae would not impede the propeller's travel. This test proved to us that the performed specifications were successful.

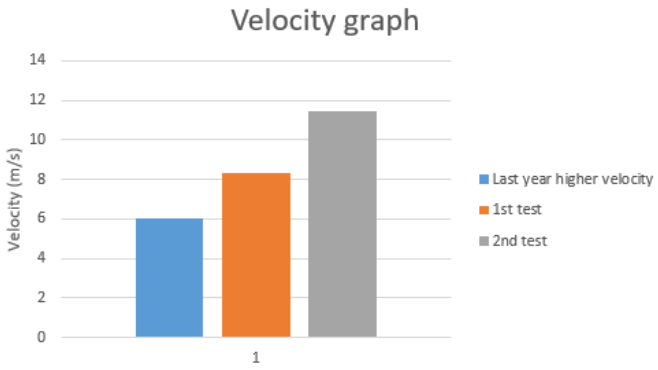

Figure 18: Boat's velocity from last year vs. this year.

B. Endurance Propeller

1) Current Design**:** Initially the team had only one propeller, which was used, for every event in the previous competition Solar Splash 2016. The mention propeller performed at an average ship speed of 2.05 m/s achieving a total of 27 laps. Although it served its purpose it was theorized that another could be more adequate and efficient. Therefore, it was proposed to create a propeller for the Endurance event in the Solar Splash 2017, which would be more effective in order to increase competitiveness.

2) Analysis of Design Concepts: The design process began by comparing a 2 bladed geometry versus a more common 3 bladed geometry. In a 3-bladed geometry the blades are closer to each other and each blade travels in the wake of the previous one, thus disturbing more the fluid. 3 blades propeller are less efficient than 2 blades, but at the same time 2 blades propeller require bigger geometry. The decision was made regarding 3 factors; thrust, efficiency, and size. For the endurance event the speed desired could not exceed 4 (m/s), and thrust will not exceed 320

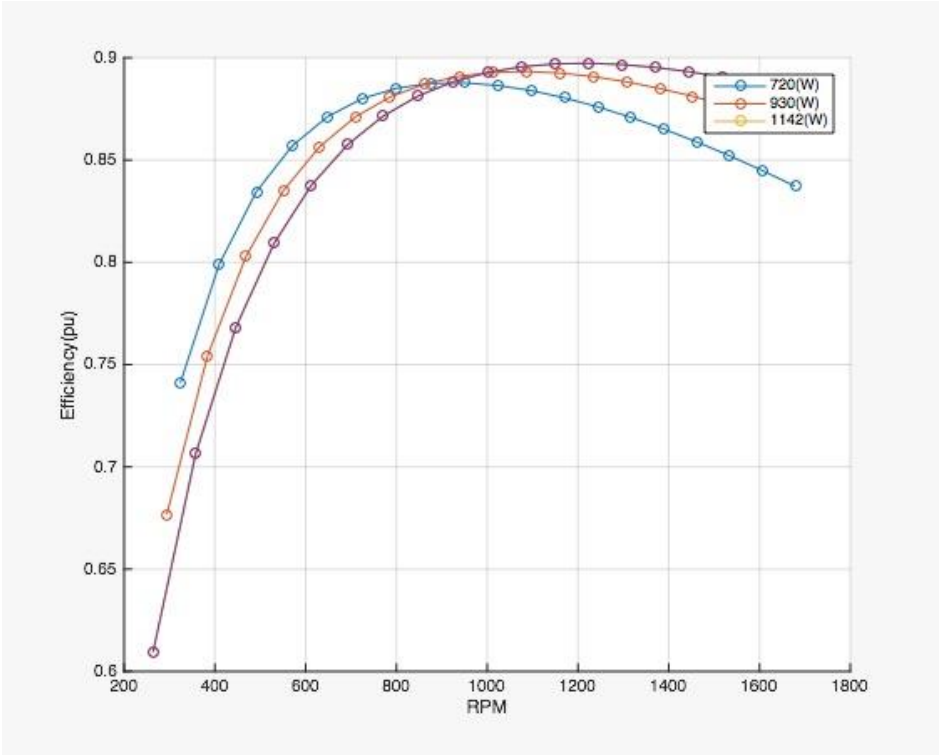

Figure18: Motor's efficiency versus rotational velocity

(N). Then, for the competition, the 2-blade propeller should result more adequate for the purpose, given the fact that the required thrust is a low value and efficiency will be higher.

The design parameters considered for the next stage, were rotational velocity, power, ship speed and hull drag along with propeller thrust, diameter and efficiency. An extensive comparison was made between a wide range of possibilities including designs at 0%, 40%, and 80% solar power gain. These designs were created using Fig. 18 considering the motor's most efficient rotational velocities and operating voltage, to avoid the depletion of the batteries before the 2-hour mark. The resulted designs are resumed in **Table 4**, considering 0% solar power gain. The remaining tables at 40% and 80% can be found in Appendix E.

Table 4: Propeller design considerations

Power-0%									
Diameter [m]	**0.30**			**0.35**			**0.40**		
Advance Coefficient	0.80	0.75	0.70	0.8	0.75	***0.7***	0.80	0.75	0.70
Volts[V]	9.5	10	11	8.5	9	***9.5***	7.5	8	8.5
Rotational Vel [rpm]	609.93	648.66	725.23	531.33	570.47	***609.93***	450.71	490.83	531.33
Drag Force [N]	141.72	141.07	150.84	145.37	146.87	***146.39***	138.71	143.04	145.37
Velocity [m/s]	2.44	2.43	2.54	2.48	2.5	***2.49***	2.4	2.45	2.48
Power$_1$ [W]	345.80	342.80	383.13	360.52	367.18	***364.51***	332.90	350.45	360.52
Propeller Efficiency	0.71	0.72	0.73	0.76	0.76	***0.76***	0.78	0.78	0.77
Power$_2$ [W]	487.04	476.11	524.84	474.37	483.13	***479.62***	426.8	449.29	468.20
Box Efficiency	0.85								
Power$_{required}$ [W]	572.99	560.13	617.46	558.08	568.38	***564.26***	502.12	528.58	550.83
Power$_{supplied}$ [W]	622.79	627.34	633.69	609.89	620.12	***622.79***	589.57	604.24	609.89
Margin [W]	49.80	67.21	16.23	51.81	51.74	***58.53***	87.45	75.66	59.06

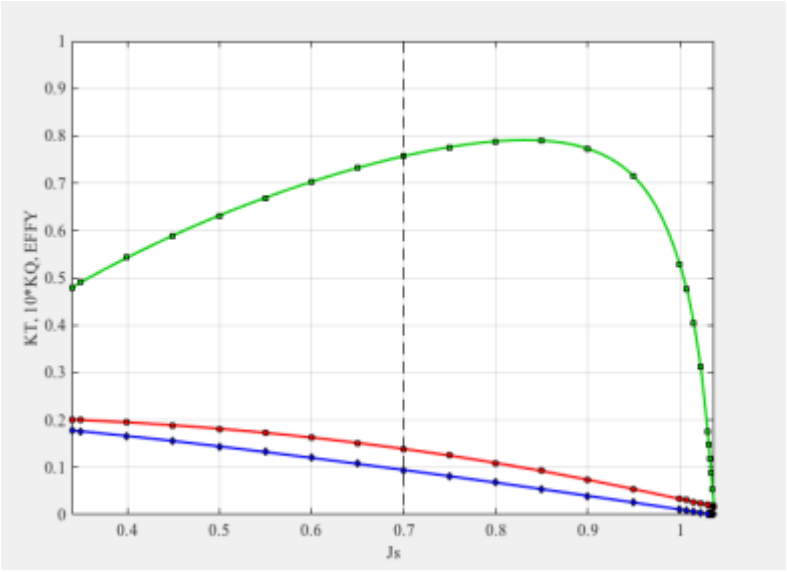

Figure 19: Performance curves for marine propeller

After selecting the most appropriate design for the task, Matlab's OpenProp was used to further analyze the desired propeller. Fig. 19 presents the performance curves for the propeller. While the behavior is as expected the coefficients of thrust and torque are considerably low. This is due to the values of thrust and torque designed for. Table 5 resumes the operating point seen in Fig 19

Table 5: Propeller point of operation

Resulted Coefficients	
Advance coefficient (J)	0.70
Thrust coefficient (KT)	0.095
Torque coefficient (KQ)	0.014
Efficiency	76%

Afterwards the resulted geometry seen in Fig. 20 was used for exportation and CAD creation using NX11. The resulted CAD was then used to manufacture the propeller using a 3-axis CNC machine. The resulted propeller is expected to create a ship speed of 2.99 m/s while rotating at 733 rpm, generating a thrust of 197 N and while avoiding the depletion of the batteries before the 2-hour mark. This performance is expected with 80% solar power.

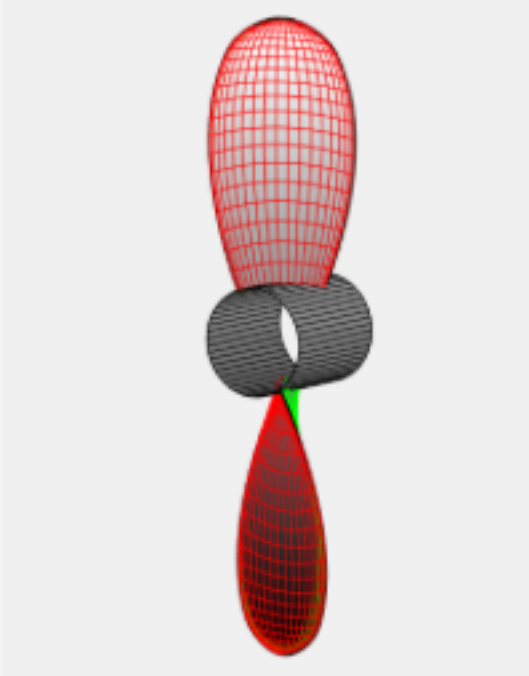

Figure 20: Propeller 3D Geometry

3) Design Testing and Evaluation: Table 6 presents the resulted propeller made out of aluminum 6061 chosen because it is inexpensive, light weight and machinable. The resulted propeller was then evaluated through a series of tests to determine it's actual performance in comparison to the theoretical performance.

Table 6: Performance Comparison

Performance	Theoretical	Experimental
Advance Coefficient (J)	0.7	0.63
Rotational Velocity [rpm]	609.93	609.93
Velocity	2.49	2.24

The error percentage calculated was 10.04%. Then, assuming the same weather conditions and functionality, as the previous competition the expected velocity of the propeller is 2.98m/s. Meaning a 45.4% speed increment that translates to a total of 39 laps for the Endurance event. A total of 12 additional laps compared to the previous competition total of 27 laps.

VII. Data Acquisition and Communications

1) Current Design: Boricua Sun's previous hydrofoil design required a complex hard real-time embedded hardware and software design. It characterized the boat's current state variables of raw, pitch, yaw, speed, RPM and height, using these measurements as input variables in a 11 variable control system that calculated the action angles of three hydrofoils to obtain optimal lift and stability. The 2016 system's data acquisition, based on a Tiva C MCU platform along with a Xbee wireless transmitter, exhibited poor reliability in the wireless communication and did not provide for local data storage. After drifting our focus away from a hydrofoil system, a real-time embedded control system was no longer needed. The traditional navigation system approach adopted this year favored a sensor network system and wireless data transmission solely for characterization and validation purposes.

A simpler printed circuit board (PCB), hosting the electrical conditioning circuits is now required for proper signal monitoring of system's voltages and currents, motor's rpm, and boat's velocity. Measurements of current and voltage for both motor and battery bank, speed, and motor RPM are necessary to ensure that the boat is working properly according to the point of operation. Compiled data is then transmitted to land real time via Wi-Fi communication to be analyzed by our team.

2) Analysis of design and concepts: Fig. 21 is a high level representation of the current data acquisition design. Development was based around a LabJack T7-Pro data acquisition device. A sensing PCB was designed to filter and condition the incoming signals. The device senses, logs, and transfers wirelessly the following measurements: motor voltage, motor current, battery bank voltage, battery bank current, boat speed, and motor RPM. Voltages and currents are sensed from a voltage signal with the device's internal Analog to Digital Converters (ADC) while speed and RPM are sensed as logic pulses and analyzed in software. In a black box sense, the system is like our previous design with the Tiva C, but the tradeoffs are: a local log saved directly to an internal SD card, augmented precision 16-bit ADCs, an embedded Wi-Fi router, and a robust set of software libraries. This means we can sense data, store it and graph it in real time with minimal in-house software development. The current design's main limitation is a set bound of 64kB of heap for local running user code. Our current design has ports available to add additional devices if needed.

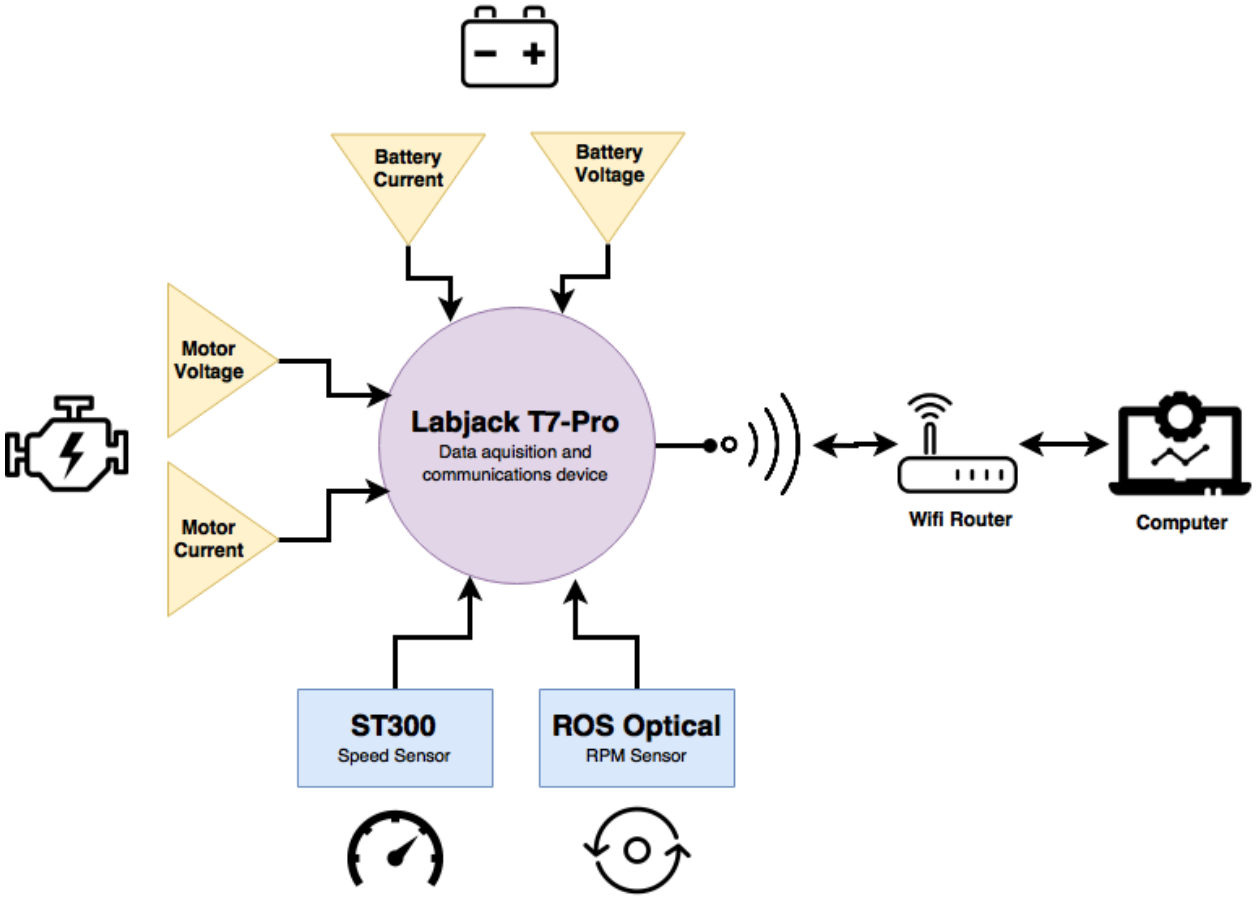

Figure 21: Boricua Sun's 2017 high level data acquisition and communications design

The boat's propulsion system consists primarily of a battery bank, motor controller and the motor. For both the endurance and sprint competition, parameters such as motor and battery voltage, current, speed, and RPM are variables that need to be monitored to ensure that the maximum performance is being achieved in any scenario. An electrical circuit was designed (Fig. 22) for signal conditioning using several differential operational amplifiers.

When measuring analog signals on a circuit with a single reference to ground, usually a simple voltage divider may suffice, depending on the maximum voltage range the microcontroller can read from its ports. The maximum voltage the Labjack can measure without damage to the unit is 10V. The voltage range measured on the boat can vary from 24V to 36V on the batteries and up to 52V on the motor, but since both ground connections cannot connect directly into the microcontroller, AD629ANZ differential operational amplifiers(OP-AMPS) were needed.

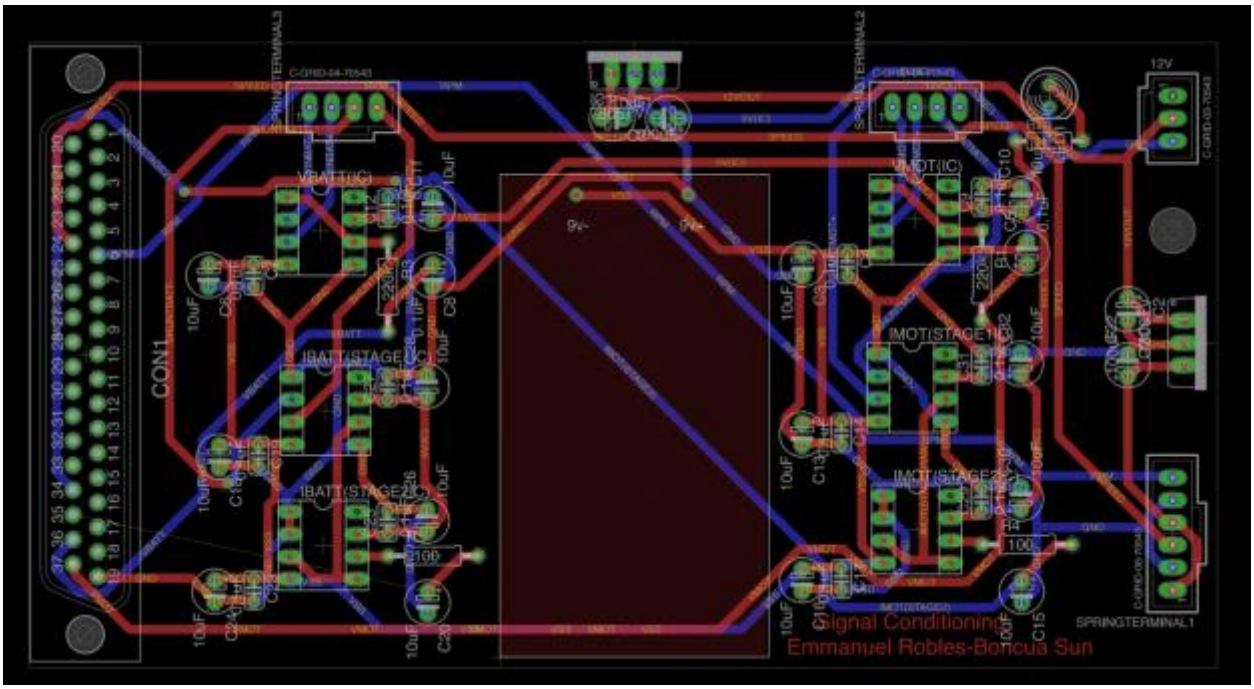

Figure 22: Sensing PCB design for signal conditioning.

The signal conditioning PCB consists of six differential operational amplifiers (Analog Devices model AD629ANZ) as well as four RC filters. This amplifier was chosen for its high common mode voltage range, versatility, easily variation of internal gain, and its reliability.

For voltage measurements, the op-amps receive a differential voltage and change the signal into a single ended output with respect to the op-amp's ground multiplied by a gain of 1/19. To measure current, a more complex circuit was developed. Shunt resistors were added in series between the battery and the motor controller (the system's input current), and between the controller and the motor (the system's output current). These resistors is rated to withstand currents up to 400Amps. Our Kelly motor controller uses high power MOSFET's that switch at 16.6KHz and vary a duty cycle of a PWM signal to control the average voltage the motor receives. As the duty cycle on the voltage varies, so does the current passing through the resistor. In theory, the signal across the resistor would also have the same duty cycle as the voltage, but with a small voltage drop measured in millivolts. The current passing through the shunt can be calculated using Ohm's Law, measuring the voltage across the resistor. The AD629ANZ has a small signal bandwidth of 500kHz when configured for a gain of 1. When configured as a non-inverting amplifier with a gain of 20, the small signal bandwidth decreases by a factor of 20 to 25 kHz. This frequency is too close to the frequency of operation of the motor controller, which results in a signal that does not stabilize fast enough at duty cycles below 50%. To increase the resolution at which the Labjack obtains this small voltage drop, two stages of amplification was implemented. Stage 1 converts the small differential voltage drop across the resistor into a single ended output of gain 1 with respect to the microcontroller's ground. Stage 2 then amplifies by a gain of 20 the signal

from stage 1, thus increasing the resolution at which the Labjack measures the voltage drop. Table 7 shows theoretical input and output signal ranges after being conditioned by the PCB.

Table 7: Theoretical signal input/output conditioning factors and ranges.

Measured variable	Raw signal range	Conditioning factor	Conditioned voltage range
Motor Voltage	0-52 V	X 1/19	0-2.737 V
Motor Current	0-75mV	X 20	0-1.500 V
Battery Voltage	24-36V	X 1/19	0-1.895 V
Battery Current	0-75mV	X 20	0-1.500 V

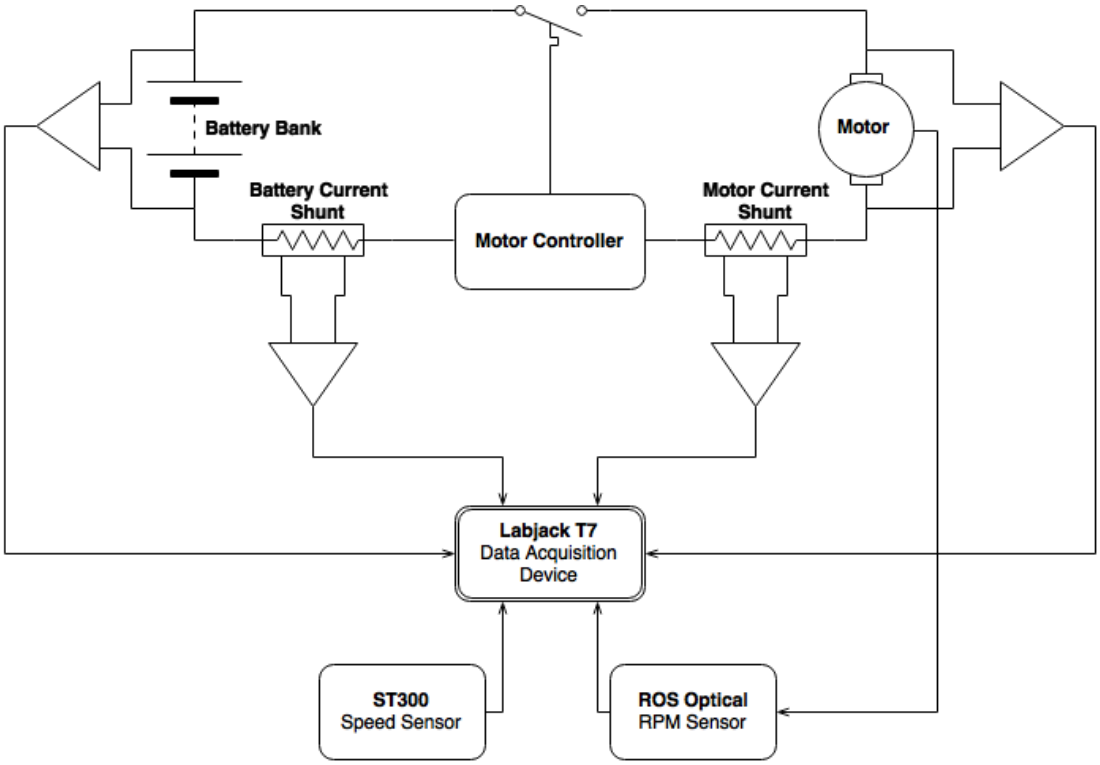

Figure 23: High level sensing electrical schematic

Monitoring the efficiency of the system for the endurance race is vital to maintain the boat's most efficient point of operation, as well as monitoring the maximum power transfer for the sprint from a standstill to full speed.

3) Design testing and evaluation: Several iterations of the circuit were made before obtaining the final, fully functional result (see Fig. 23). Initially, each measurement done with the PCB was tested individually on a controlled environment using digital multimeter's and signal generators.

For voltage measurements, the AD629ANZ was used since the first iteration. During laboratory testing, measurements made with our test system were working accurately according to the manufacturer's specifications. When testing the circuitry to measure

voltage on the boat, a low pass RC filter had to be implemented to ignore low frequency noise that was affecting the reading. After the filter, voltage readings greatly improved, obtaining readings with a final resolution of ± 0.6V.

Two differential operational amplifiers were tested to measure current using shunt resistors: the Texas Instruments LMP8602, with a fixed gain of 50V/V, and the AD629ANZ configured for a fixed gain of 20V/V. The AD629 was chosen at the end since measurements were far more reliable when tested on our final system.

Initially, a single stage circuit was implemented with the AD629ANZ, receiving the differential voltage from the shunt resistor and amplifying it by a gain of 20. When testing if the circuit adequately processed the shunt's voltage drop, the oscilloscope reading showed that the signal did not stabilize fast enough at relatively low duty cycles, as shown on Fig. 24 below:

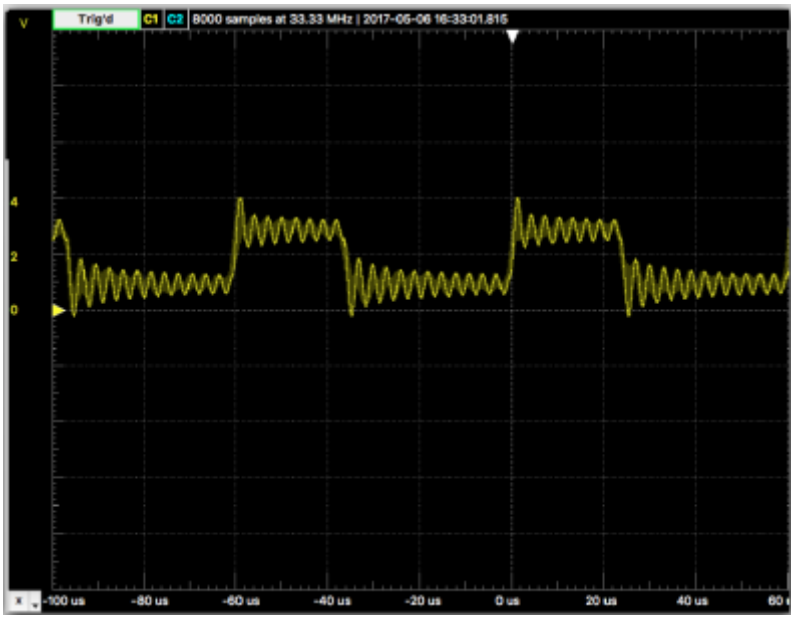

Figure 24: Conditioned shunt resistor signal not stabilized fast enough at 50% duty cycle.

An additional stage had to be implemented before amplifying the signal, as well as a low pass RC filter. This was due to the small signal bandwidth of the OP-AMP configured for gain 20. After adding this additional stage for current measurement, resolution varied from 1% to 2% from the actual reading using a clamp meter, as shown in Fig. 25 below:

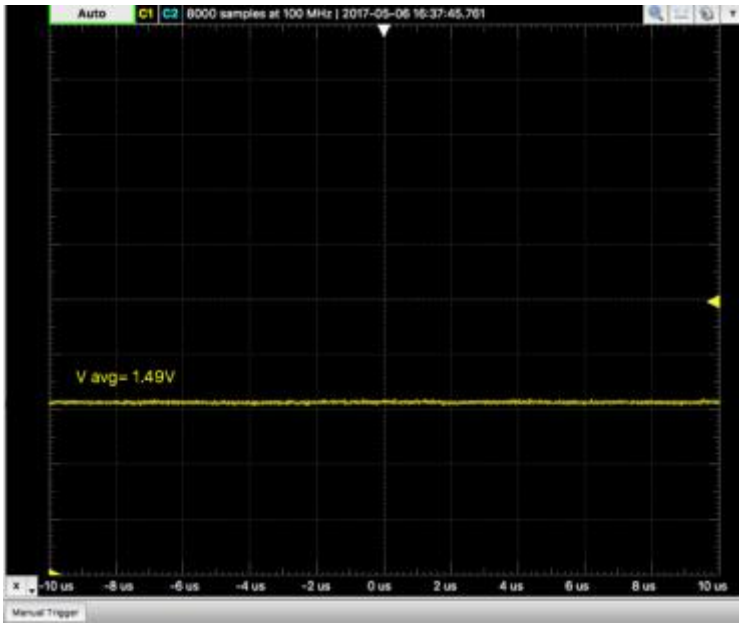

Figure 25: Stabilized measurements from shunt resistor at 50% duty cycle.

After every measurement on the boat was successfully conditioned on a breadboard, a prototyping board was developed and its the working circuit right now. We will be manufacturing a final PCB for when the competition arrives.

Data logged and transferred using the Labjack was validated using external tools on the devices input nodes. A Fluke 114 electrical multimeter's voltage measurements for the motor and battery bank's current and voltages were compared to the Labjack's measurements. A Strobette Model 1000 tachometer was used to validate our RPM measurement. To test the system in time, we ran the Labjack with the PCB and confirmed that the incoming signals were not saturated or with noise. The Labjack ran for approximately 2.5 hours to see if the code gave any heap memory issues and Wi-Fi communication was tested on land.

For future versions of this circuit, there are three main areas where it can be improved. Current and voltage measurements for solar panels need to be added on the circuit's next iteration and the circuit's resolution can further be improved designing a series of filters. Also, a display showing real time measurements to the boat's driver can later on be installed.

VIII. Project Management

The Boricua Sun is an undergraduate team sponsored primarily by private companies such as General Motors, Abbot, and Boeing, along with UPRM through the Industries Affiliate Program of the ECE Department and the Engineering Dean. Team members of all academic years and several disciplines (refer to Appendix D – Table D-1) encompassed a natural balance of experience, knowledge, desire, drive, and determination. The UPRM is represented through four Engineering Programs: Electrical, Computer, Chemical, and Mechanical. The senior members guided by the captain, Mr. Alexander Santos, through the sub-team's structure adopted (Solar System, Electrical, Mechanical, Data Acquisition) mentored and guided the younger unexperienced students. Such scheme along with an annual recruitment info session enables team continuity and sustainability for the years to come.

Figure 26: Web based collaborative mind mapping

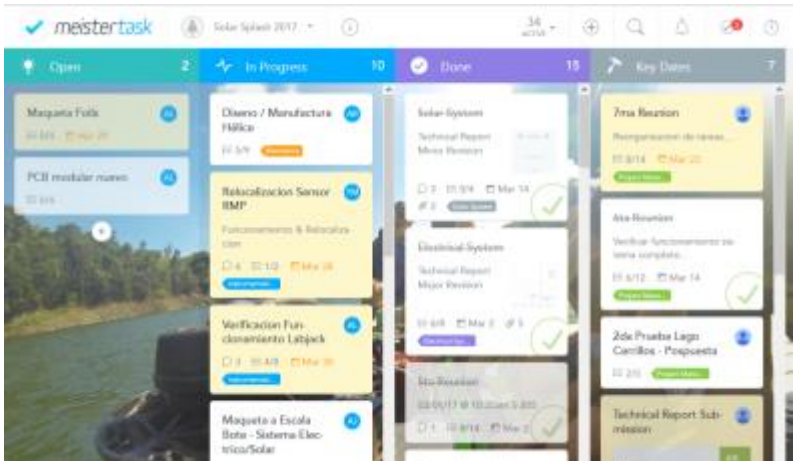

Figure 27: Online project and task management tool

Regarding the project management, this year the Boricua Sun adopted the use of 1) a web based collaborative mind mapping, MindMeister, and 2) an online project and task management solution, MeisterTask. Initially, MindMeister enabled effective online collaboration of the whole team in the definition of the overall team and sub-team objectives through an interactive visual platform (refer to Fig. 26) . Afterwards, each member defined all the associated tasks required to complete each objective. MeisterTask provided a highly effective web-based solution that enabled team communication, scheduling, time management, and task assessment accessible to all members always (see Fig. 27). The use of this web-based platforms greatly increased the team's productivity and diminished management difficulties.

IX. Conclusions and Recommendations

The Boricua Sun Team performed a lesson learned analysis following the 2016 Solar Splash Event. The main findings of the analysis were implemented as the objectives for this year. One of the most significant findings led to the postposition of the Hydrofoil System Implementation given the fundamental issues that needed to be addressed before implementing such a system. The following section summarizes the results obtained in preparation for the 2017 Solar Splash Event.

Endurance: For this event a new propeller, new solar panel and new batteries were specified. The solar panel has been fabricated ant the team is in the process of characterization of the device. The propeller was fabricated and tested. Preliminary performance indicated a speed of 2.5 m/s (33 laps) at the desired two-hour battery discharge without solar panels.

Sprint: For this event, a new power system was designed and implemented, a new (shorter) midsection for the drivetrain along with corresponding shaft and new batteries were specified. A dc-dc boost converter with a matching sprint propeller is currently under development and might be ready on time for the competition. The preliminary performance registered a reduction of 26 seconds from the 2016 results. The expected sprint time is 29 second.

Table 8: Boricua Sun's competition score assessment.

Category	2016 Rank	2016 Points	Expected Rank	Expected Points
Endurance	6th	289/400	1st	400/400
Sprint	7th	108/250	3rd	158/250
Slalom	6th	39/100	2nd	68/100
Others(mfg,report,visual, qualifiers)	N/A	148/250	N/A	175/250
Overall	9th	584/1000	Top-Three	801/1000

Other goals achieved were weight reduction, enhanced data acquisition as well as visual presentation of the system. Table 8 presents a points analysis based on 2016 results and the expected performance given the enhancements in preparation for the competition. The Boricua Sun Team has a chance of a Top-Three performance this year.

Overall the team is very excited about this year possibilities. There's always room for improvement in many areas of the project. However, project management, fund raising and transportation coordination continue to present real challenges to the team.

Appendix A: Battery Documentation

This year two Odyssey Extreme PC1100 and two Odyssey Extreme PC950 were utilized in the bank for a total weight of 95lbs.

MODEL	Voltage	PHCA** (5 sec.)	CCA*	HCA	MCA	Nominal Capacity (20 Hr Rate-Ah)	Nominal Capacity (10 Hr Rate-Ah)	Reserve Capacity Minutes	Length inches (mm)	Width inches (mm)	Height inches (mm)	Weight lbs (kg)	Terminal	Torque Specs in-lbs (Nm max)	Internal Resistance (mΩ)	Short Circuit Current
 **PC950**	12	950	400	600	500	34	32	60	9.8 (250.0)	3.8 (97.0)	6.1 (156.0)	20.0 (9.0)	M6 Stud	35 (3.9)	7.1	1700A
 PC1100	12	1100	500	800	650	45	43	87	9.8 (250.0)	3.8 (97.0)	8.1 (206.0)	27.5 (12.5)	M6 Stud	35 (3.9)	5.1	2450A

Table A1: Manufacturer's battery specifications

*Cold Start Performance S.A.E J537 JUNE 82
**Pulse Current
† Can be fitted with brass automotive terminal
Optional metal jackets available on PC545, PC680, PC925, PC1200, PC1700 and 31-PC2150
Operating temperature range:
PC950 and PC1100: -40°F (-40°C) to 122°F (50°C)

MSDS

Section I - Product and Manufacturer Identity

Product Identity:
Sealed Lead Battery
Cyclon®, Genesis®, SBS, SBS J, Hawker XE™ Odyssey® or Trolling Thunder™

Manufacturer's Name and Address:
EnerSys Energy Products Inc. (formerly Hawker Energy Products Inc.)
617 North Ridgeview Drive
Warrensburg, MO 64093-9301
Emergency Telephone Number: (660) 429-2165
Customer Service Telephone Number: 800-964-2837

Section II - Ingredients

Hazardous Components	CAS #	OSHA PEL-TWA	% (By weight)
Lead	7439-92-1	50µg/m3	45 - 60 %
Lead Dioxide	1309-60-0	50µg/m3	15 - 25 %
Sulfuric Acid Electrolyte	7664-93-9	1.0 mg/m3	15 - 20 %
Non-Hazardous Materials	N/A	N/A	5 - 10 %

Section III - Physical/Chemical Characteristics

Boiling Point - N/A Specific Gravity (H2O=1) - NA
Vapor Pressure (mm Hg.) - N/A Melting Point - N/A
Solubility in Water - N/A Appearance & Color - N/A

Section IV - Fire & Explosion Hazard Data

Flash Point (Method Used): N/A **Flammable Limits**: N/A **LEL**: N/A **UEL**: N/A

Extinguishing Media:
Multipurpose Dry chemical, CO2 or water spray.

Special Fire Fighting Procedures:
Cool Battery exterior to prevent rupture. Acid mists and vapors in a fire are toxic and corrosive. Unusual Fire and Explosion Hazards: Hydrogen gas may be produced and may explode if ignited. Remove all sources of ignition.

Section V - Reactivity Data and Shipping/Handling Electrical Safety

Conditions to Avoid: Avoid shorting, high levels of short circuit current can be developed across the battery terminals. Do not rest tools or cables on the battery. Avoid over-charging. Use only approved charging methods. Do not charge in gas tight containers.

Requirements for Safe Shipping and Handling of Cyclon® Cells: Warning – Electrical Fire Hazard – Protect Against Shorting

- Terminals can short and cause a fire if not insulated during shipping.
- Cyclon® product must be labeled "NONSPILLABLE" during shipping. Follow all federal shipping regulations. See section IX of this sheet and CFR 49 Parts 171 through 180, available anytime online at wwww.gpoaccess.gov.

Requirements for Shipping Cyclon® Product as Single Cells

- Protective caps or other durable inert material must be used to insulate each terminal of each cell unless cells are shipping in the original packaging from EnerSys, in full box quantities.
- Protective caps are available for all cell sizes by contacting EnerSys Customer Service at 1-800-964-2837.

Requirements for Shipping Cyclon® Product Assembled Into Multicell Batteries

- Assembled batteries must have short circuit protection during shipping.
- Exposed terminals, connectors, or lead wires must be insulated with a durable inert material to prevent exposure during shipping.

Section VI - Health Hazard Data

Routes of Entry: N/A

Health Hazards (Acute & Chronic): N/A

Emergency & First Aid Procedures:
Battery contains acid electrolyte which is absorbed in the separator material. If battery case is punctured, completely flush any released material from skin or eyes with water.

Proposition 65:
Warning: Battery posts, terminals and related accessories contain lead and lead compounds, chemicals known to the State of California to cause cancer and reproductive harm. Batteries also contain other chemicals known to the State of California to cause cancer. Wash hands after handling.

Section VII - Product and Manufacturer Identity

Steps to be taken in case material is released or spilled:
Avoid contact with acid materials. Use soda ash or lime to neutralize. Flush with water.

Waste Disposal Method:
Dispose of in accordance with Federal, State, & Local Regulations. Do not incinerate. Batteries should be shipped to a reclamation facility for recovery of the metal and plastic components as the proper method of waste management. Contact distributor for appropriate product return procedures.

Section VIII - Control Measures - Not Applicable

Section IX - Transportation, Shipping and Handling

EnerSys Energy Products Inc. batteries are starved electrolyte batteries which means the electrolyte is absorbed in the separator material. The batteries are also sealed. As of September 30, 1995, EnerSys Energy Products Inc. batteries were classified as "nonspillable batteries", and as such are not subject to the full requirements of 49 CFR § 173.159. The previous exempt classification, "Dry Batteries, Not Restricted" was discontinued effective September 30, 1995. "Nonspillable" batteries are excepted from the regulation's comprehensive packaging requirements if the following conditions are satisfied: (1) The battery is protected against short circuits and is securely packaged. (2) For batteries manufactured after September 30, 1995, the battery and outer packaging must be plainly and durably marked "NONSPILLABLE" or "NONSPILLABLE BATTERY". (3) The battery is capable of withstanding vibration and pressure differential tests specified in 49 CFR § 173.159(d). (4) At a temperature of 55 ºC (131ºF), the battery must not contain any unabsorbed free-flowing liquids, and is designed so that electrolyte will not flow from a ruptured or cracked case.

EnerSys Energy Products Inc. batteries have been tested by WYLE Scientific Services & Systems Laboratories Group and determined to be in compliance with the vibration and pressure differential tests contained in 49 CFR § 173.159(d), and therefore as of September 30, 1995, excepted from the DOT requirements set forth in 49 CFR § 173.159, other than paragraph (d).

Battery shipments from EnerSys Energy Products Inc. Warrensburg location, will be properly labeled in accordance with applicable DOT regulations.

Packaging changes performed at other locations may require additional labeling, since in addition to the battery itself containing the required marking, the outer packaging of the battery must also contain the required marking: "NONSPILLABLE" OR "NONSPILLABLE BATTERY". Because the batteries are classified as "Nonspillable" and meet the three conditions above, [from § 173.159(d)] they do not have an assigned UN number nor do they require additional DOT hazard labeling.

The regulation change effective September, 1995, was to clarify and distinguish to shippers and transporters, all batteries that have been tested and determined to be in compliance with the DOT Hazardous Material Regulations, the International Civil Aeronautics Organization (ICAO), and the International Air Transport Association (IATA) Packing Instruction 806 and Special Provision A67, and therefore excepted from all other requirements of the regulations and classified as a "nonspillable battery".

Per 42 USC Section 14322 (US Code Title 42 – The Public Health and Welfare), packaging must be marked with the following: "Contains Sealed Lead Battery" and "Battery Must Be Recycled".

Section X - Additional Information

The EnerSys Energy Products Inc. sealed lead acid battery is determined to be an "article" according to the OSHA Hazard Communication Standard and is thereby excluded from any requirements of the standard. The Material Safety Data Sheet is therefore supplied for informational purposes only.

The information and recommendations contained herein have been compiled from sources believed to be reliable and represent current opinion on the subject. No warranty, guarantee, or representation is made by EnerSys Energy Products Inc., as to the absolute correctness or sufficiency of any representation contained herein and EnerSys Energy Products Inc. assumes no responsibility in connection therewith, nor can it be assumed that all acceptable safety measures are contained herein, or that additional measures may not be required under particular or exceptional conditions or circumstances.

N/A or Not Applicable - Not applicable for finished product used in normal conditions.
Informational MSDS Part Number 2602-0043 Rev. 2 (09/07/06)

Appendix B: Flotation Calculations

The buoyancy force is given by the specific weight times the volume of the component, to comply with Rule 7.14.2 a 20 % increase in weight was added. Table B2 shows the total weight and the total buoyancy force of the boat. The total Buoyancy Force for both Sprint and Endurance configurations has a higher magnitude than the total weight with 20% safety factor.

Specific Weight (lbf/ft^3)
62.2

Table B1: Boricua Sun's specific weight

Component	Weight (lbf.)	SF * Weight (lbf.)	Volume (ft^3)	Buoyancy Force (lbf.)
Drive Train Pivot	3.5	4.2	0.01	0.622
Propeller with transmission	5.9	7.08	0.06	3.732
Chair	2	2.4	0.05	3.11
Batteries	100	120	0.4	24.88
Steering System (with box)	23.5	28.2	0.6	37.32
Motor Assembly	50.6	60.72	0.2	12.44
Hull	77	92.4	14.1	877.02
Controllers	55.4	66.48	0.07	4.354
Driver	150	180	0	0
Solar Array	28	33.6	3.5	217.7
Sum for Sprint	495.9	**595.08**	18.99	**1181.178**
Sum for Endurance	467.9	**561.48**	15.49	**963.478**

Table B2: Flotation calculations spreadsheet

Appendix C: Proof of Insurance

ACORD™ CERTIFICATE OF LIABILITY INSURANCE

DATE (MM/DD/YYYY): 5/5/2017

PRODUCER (787) 721-4444 FAX (787) 722-4894

GLOBAL INSURANCE AGENCY INC
257 RECINTO SUR ST. 2ND FLOOR
PO BOX 9023918
SAN JUAN, PR 00902-3918

THIS CERTIFICATE AS A MATTER OF INFORMATION ONLY AND CONFERS NO RIGHTS UPON THE CERTIFICATE HOLDER. THIS CERTFIFICATE DOES NOT AMEND, EXTENDED OR ALTER THE COVERAGE AFFORDED BY THE POLICIES BELOW.

INSURER AFFORDING COVERAGE		NAIC#
INSURER A	TRIPLE S PROPIEDAD	130
INSURER B		
INSURER C		
INSURER D		
INSURED E		

INSURED
UNIVERSIDAD DE PUERTO RICO
ADMINISTRACIÓN CENTRAL
JARDÍN BOTÁNICO SUR
118 CALLE FLAMBOYÁN
SAN JUAN PR 00926-1117

COVERAGES

THIS POLICY OF INSURANCE LITED BELOW HAVE BEEN ISSUED TO THE INSURED NAMED ABOVE FOR THE POLICY PERIOD INDICATED. NOTWITHSTANDING ANY REQUIREMENT, TERM OR CONDITION OF ANY CONTRACT OR OTHER DOCUMENT WITH RESPECT TO WHICH THIS CERTIFICATE MAY BE ISSUED OR MAY PERTAIN, THE INSURANCE AFFORDED BY TH POLICIES DESCRIBED HEREIN IS SUBJECT TO ALL THE TERMS, EXCLUSIONS AND CONDITIONS OF SUCH POLICIES, AGGREGATE LIMITS SHOWN MAY HAVE BEEN REDUCED BY PAID CLAIMS.

CO	A/I	TYPE OF INSURANCE	POLICY NUMBER	POLICY EFFECTIVE DATE (MM/DD/YY)	POLICY EXPIRATION DATE (MM/DD/YY)	LIMITS	
A		GENERAL LIABILITY	CL-83049539	07/01/2016	07/01/2017	EACH OCCURRENCE	$ 1,500,000
	X	COMMERCIAL GENERAL LIABILITY				DAMAGE TO RENTED PREMISES (EA OCCURRENCE)	$ 50,000
		CLAIM MADE X OCCUR				MED EXP (ANY ONE PERSON)	$ 5,000
						PERSONAL & ADV INJURY	$ 1,500,000
						GENERAL AGGREGATE	$ 3,000,000
		GEN'L AGGREGATE LIMIT APPLIES PER:				PRODUCTS –COMP/OP AGG	$ 3,000,000
		POLICY PRO-JECT LOC					$
		AUTOMOBILE LIABILITY				COMBINED SINGLE LIMIT (EA ACCIDENT)	$
		ANY AUTO				BODILY INJURY (PER PERSON)	$
		ALL OWNED AUTOS				BODILY INJURY (PER ACIDENT)	$
		SCHEDULED AUTOS				PROPERTY DAMAGE (PER ACCIDENT	$
		HIRED AUTOS					
		NON-OWNED AUTOS					
		GARAGE LIABILTY				AUTO-ONLY EA ACCIDENT	$
		ANY AUTO				OTHER THAN EA ACC	$
						AUTO ONLY: AGG	$
A		EXCESS/UMBRELLA LIABILTY	UC-67006707	07/01/2016	07/01/2017	EACH OCCURRENCE	$ 5,000,000
	X	OCCUR CLAIMS MADE				AGGREGATE	$ 5,000,000
		DEDUCTIBLE					$
	X	RETENTION $ 10,000					$
A		EMPLOYER'S LIABILITY	CL-83049539	07/01/2016	07/01/2017	WC STATUTORY LIMITS / OTHER	
						E.L. EACH ACCIDENT	$ 1,000,000
						E.L. DISEASE –EA EMPLOYEE	$ 1,000,000
						E.L DISEASE – POLICY LIMIT	$ 1,000,000
		OTHER					

DESCRPTION OF OPERATIONS / LOCATIONS/VEHICLES/EXCLUSIONS ADDED BY ENDORSEMENT / SPECIAL PROVISIONS

PERIOD: JUNE 7 - 11, 2017
PURPOSE: UNIVERSITY OF PUERTO RICO-MAYAGUEZ CAMPUS PARTICIPATION AT 2017 SOLAR SPLASH COMPETITION.
CERTIFICATE NO: 1525

CERTIFICATE HOLDER

INTERNATIONAL INTERCOLLEGIATE SOLAR/ELECTRIC BOAT REGATTA
EASTWOOD LAKE
DAYTON, OH 454041525

SHOULD ANY OF THE ABOVE DESCRIBED POLICIES BE CANCELLED BEFORE THE EXPIRATION DATE THEROF, THE ISSUING INSURERE WILL ENDEAVOR TO MAIL 30 DAYS WRITTEN NOTICE TO THE CERTIFICATE HOLDER NAMED TO THE LEFT, BUT FAILURE TO MAIL SUCH NOTICE SHALL IMPOSE NO OBLIGATION OR LIABILITY OF ANY KIND UPON THE INSURER, IT'S AGENTS OR REPRESENTATIVE.

AUTHORIZED REPRESENTATIVE

GLOBAL INSURANCE AGENCY INC

ACORD 25 (2001/08) @ACCORD CORPORATION 1988

TRIPLE-S PROPIEDAD

This endorsement, effective **6/7/2017** forms a part of policy No. **CL-83049539**

Issued to. **UNIVERSIDAD DE PUERTO RICO &/OR ET/ALS**

By TRIPLE-S PROPIEDAD

HOLD HARMLESS AGREEMENT

THE CONTRACTOR, FOR ITSELF, AGENTS, EMPLOYEES, SUCCESSOR AND ASSIGNS AGREES TO SAFE AND HOLD HARMLESS THE OWNER FROM AND AGAINST ANY AND ALL CLAIMS, DEMANDS AND/OR SUITS WHETHER JUDICIAL OR EXTRA JUDICIAL FOR ANY CAUSE WHATSOEVER ARISING OUT OF OR RELATED TO THE EXECUTION OF THE CONTRACT DESCRIBED BELOW, AND ITS INSURER SHALL DEFEND THE OWNER FROM SUCH CLAIMS, DEMANDS AND/OR SUITS AND SHALL BEAR ALL THE EXPENSES FOR SUCH DEFENSE CONTEMPLATED WITHIN THE COVERAGES AND LIMITS PROVIDED BY THE POLICY, EXCEPT WHERE SUCH CLAIMS, DEMANDS AND/OR SUITS ARE DUE SOLELY TO THE NEGLIGENCE OF THE ADDITIONAL INSURED &/OR CERTIFICATE HOLDER.

THIS HOLD HARMLESS AGREEMENT DOES NOT EXTEND, MODIFY, INCREASE LIMITS OF, OR OTHERWISE ALTER THE COVERAGE PROVIDED BY THIS POLICY.

ADDITIONAL INSURED

IT IS HEREBY UNDERSTOOD AND AGREED THAT **INTERNATIONAL INTERCOLLEGIATE SOLAR/ELECTRIC BOAT REGATTA** IS INCLUDED AS ADDITIONAL INSURED UNDER THIS POLICY WITH RESPECT TO THE REFERENCE PROJECT AND AS PER ISO FORM CG-2010 10 01 ATTACHED.

INTERNATIONAL INTERCOLLEGIATE SOLAR/ELECTRIC BOAT REGATTA
PERIOD: JUNE 7 - 11, 2017
PURPOSE: UNIVERSITY OF PUERTO RICO-MAYAGUEZ CAMPUS PARTICIPATION AT 2017 SOLAR SPLASH COMPETITION.

CANCELLATION CLAUSE

IT IS HEREBY UNDERSTOOD AND AGREED THAT IN THE EVENT OF CANCELLATION NINETY (90) DAYS PRIOR WRITTEN NOTICE SHALL BE GIVEN EXCEPT FOR NON-PAYMENT OF PREMIUM IS WHICH CASE TEN (10) DAYS PRIOR WRITTEN NOTICE SHALL BE GIVEN.

All other terms and conditions of this policy remain unchanged.

GLOBAL INSURANCE AGENCY INC
Authorized Representative

1510 Ave. F. D. Roosevelt, Guaynabo, PR 00968
PO Box 70313, San Juan, PR 00936-0313
Tel. 787-749-4600 web www.sspropiedad.com

POLICY NUMBER: CL-83049539

COMMERCIAL GENERAL LIABILITY
CG 20 10 10 01

THIS ENDORSEMENT CHANGES THE POLICY. PLEASE READ IT CAREFULLY.

ADDITIONAL INSURED – OWNERS, LESSEES OR CONTRACTORS – SCHEDULED PERSON OR ORGANIZATION

This endorsement modifies insurance provided under the following:

COMMERCIAL GENERAL LIABILITY COVERAGE PART

SCHEDULE

Name of Person or Organization:
INTERNATIONAL INTERCOLLEGIATE SOLAR/ELECTRIC BOAT REGATTA

(If no entry appears above, information required to complete this endorsement will be shown in the Declarations as applicable to this endorsement.)

A. Section II – Who Is An Insured is amended to include as an insured the person or organization shown in the Schedule, but only with respect to liability arising out of your ongoing operations performed for that insured.

B. With respect to the insurance afforded to these additional insureds, the following exclusion is added:

2. Exclusions

This insurance does not apply to "bodily injury" or "property damage" occurring after:

(1) All work, including materials, parts or equipment furnished in connection with such work, on the project (other than service, maintenance or repairs) to be performed by or on behalf of the additional insured(s) at the site of the covered operations has been completed; or

(2) That portion of "your work" out of which the injury or damage arises has been put to its intended use by any person or organization other than another contractor or subcontractor engaged in performing operations for a principal as a part of the same project.

Appendix D: Team Roster

Boricua Sun's current team is composed of 10 undergraduate students from Electrical, Mechanical, computer and Chemical Engineering mayors:

Table D-1: Boricua Sun's Current Team Members

Name	Last Names	Engineering Program	Studies Year	Team Role
Diego	Capre-Ramírez	Computer	4	Communications
Noel	Colón	Mechanical	5	Propeller and Hull designer
Ignacio	Delgado-Cay	Electrical	4	Discharge Analog Controller
José	Feliciano-Cruz	Electrical	4	Electrical System Design
Alan	López-García	Computer	9	Communications and Electronics
Yadiel	Márquez	Mechanical	5	Drive Train
Arnaldo	Rivera-Otero	Mechanical	5	Propeller and Hull designer
Emmanuel	Robles-Rivera	Electrical	4	PV System and Electronics
Amanda	Santiago-Blanco	Chemical	3	PV System
Alexander	Santos-Lozada	Electrical	8	Team Captain /Electrical Eng. Leader

Contributions by past team members where fundamental for this year's work:

Table D-2: Boricua Sun's Past Team Members

Name	Last Names	Engineering Program	Contribution Year	Team Role
Arturo	García-Palou	Mechanical	2016	Actuator System
Guillermo	García-Schmidt	Mechanical	2016	Mechanical Eng. Leader
Iván	Morales-Pérez	Electrical	2016	Power Systems
Christian	Rodríguez-Merced	Electrical	2016	Electronics
Arnaldo	Santiago-Acevedo	Mechanical	2016	Throttle, Steering and Hull

Appendix E: Power design tables

Power-40%									
Diameter [m]	**0.30**			**0.35**			**0.40**		
Advance Coefficient	0.80	0.75	0.70	0.8	0.75	0.7	0.80	0.75	0.70
Volts [V]	10.5	11.5	12	9.5	10	11.5	8.5	9.0	9.5
Rotational Vel [rpm]	670.2	747.75	786.11	591.27	630.93	670.2	510.48	551.15	591.27
Drag Force [N]	164.5	176.82	171.51	172.3	172.41	170.04	168.64	171.94	172.3
Velocity [m/s]	2.68	2.8	2.75	2.76	2.76	2.74	2.72	2.76	2.76
$Power_1$ [W]	440.86	495.10	471.65	475.55	475.85	465.91	458.70	474.55	475.55
Propeller Efficiency	0.72	0.73	0.73	0.76	0.76	0.76	0.78	0.78	0.77
$Power_2$ [W]	612.31	678.21	646.10	625.72	626.12	613.04	588.08	608.40	617.59
Box Efficiency	0.85								
$Power_{required}$ [W]	720.36	797.90	760.12	736.14	736.61	721.22	691.86	715.77	726.58
$Power_{supplied}$ [W]	802.41	813.44	817.48	786.08	795.04	802.41	761.90	775.19	786.09
Margin [W]	82.05	15.54	57.36	49.94	58.43	81.19	70.04	59.42	59.51

Table E1: 40% Solar Power Table

Power-80%									
Diameter [m]	**0.30**			**0.35**			**0.40**		
Advance Coefficient	0.80	0.75	0.70	0.8	0.75	0.7	0.80	0.75	0.70
Volts [V]	11.5	12.5	12.0	10.5	11	11.5	9.5	10	10.5
Rotational Vel [rpm]	732.78	810.48	848.94	653.81	695.19	732.78	573.16	613.72	653.81
Drag Force [N]	189.97	201.54	194.23	202.82	201.77	196.46	203.45	204.73	202.82
Velocity [m/s]	2.93	3.04	2.97	3.05	3.04	2.99	3.06	3.07	3.06
$Power_1$ [W]	556.61	612.68	576.86	618.60	613.38	587.42	622.56	628.52	620.63
Propeller Efficiency	0.73	0.73	0.74	0.76	0.76	0.76	0.78	0.78	0.77
$Power_2$ [W]	762.48	839.29	779.54	813.95	807.08	772.92	798.15	805.80	806.01
Box Efficiency	0.85								
$Power_{required}$ [W]	897.04	987.40	917.11	957.59	949.51	909.31	939.0	948.00	948.25
$Power_{supplied}$ [W]	978.44	991.51	996.49	959.94	969.99	978.44	933.65	947.96	959.94
Margin [W]	81.40	4.11	79.38	2.35	20.48	69.13	-5.35	-0.04	11.69

Table E2: 80% Solar Power Table

Appendix F: DC /DC Boost Converter

I. Boost Converter Equations:

$$V_{in} = 36V, \;\; V_o = 52V, \;\; , Io = 280A, f = 100kHz$$

$$D = 1 - \frac{Vin}{Vo} = 1 - \frac{36}{52} = .31$$

$$Po = Vo * Io = 52(280) = 14.56kW$$

$$R_L = \frac{Vo}{Io} = \frac{52}{280} = .1857\Omega$$

$$I_L \geq \frac{Vo * Io}{Vin} = \frac{52(280)}{36} = 404.44A$$

$$\Delta\, i_L = \frac{Vo * Io * 0.2}{Vin} = \frac{52(280)0.2}{36} = 80.88A$$

$$L > \frac{Vin(Vout - Vin)}{\Delta\, i_L * f * Vout} = \frac{36(52 - 36)}{81 * 100k * 52} = 1.37uH$$

$$C \geq \frac{Ioutmax * D}{\Delta\, Vo * f} = \frac{280 * 0.31}{0.5 * 100k} \geq 1.8mF$$

II. Simulink Simulation:

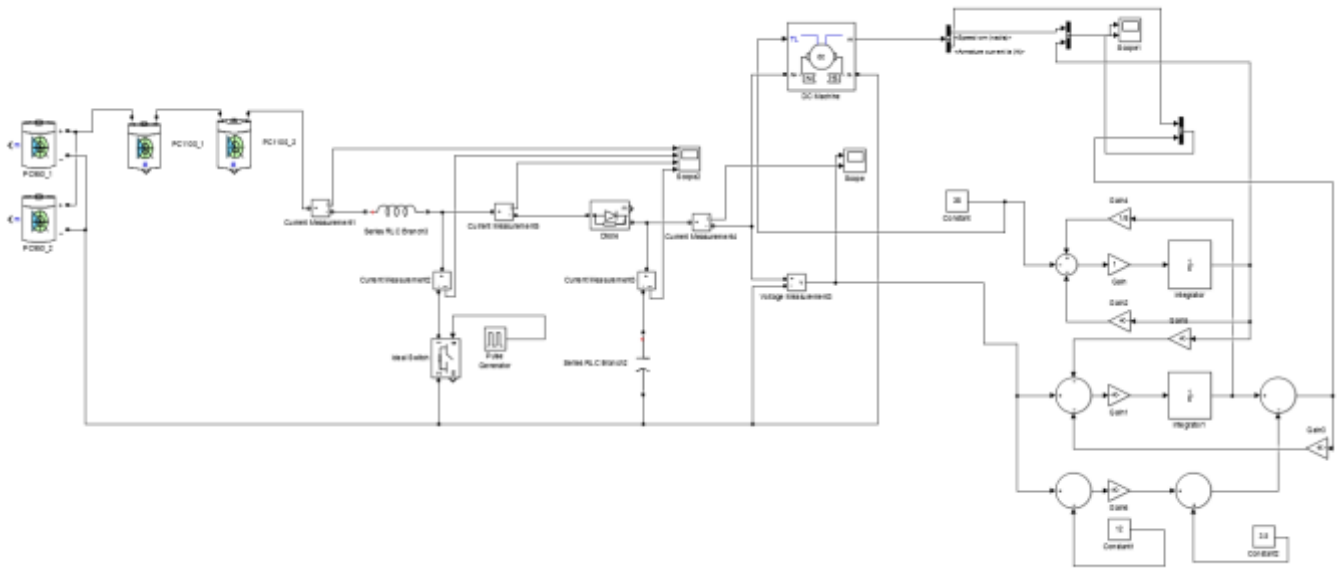

Fig. F1: Boost converter simulation in Matlab with motor and battery model

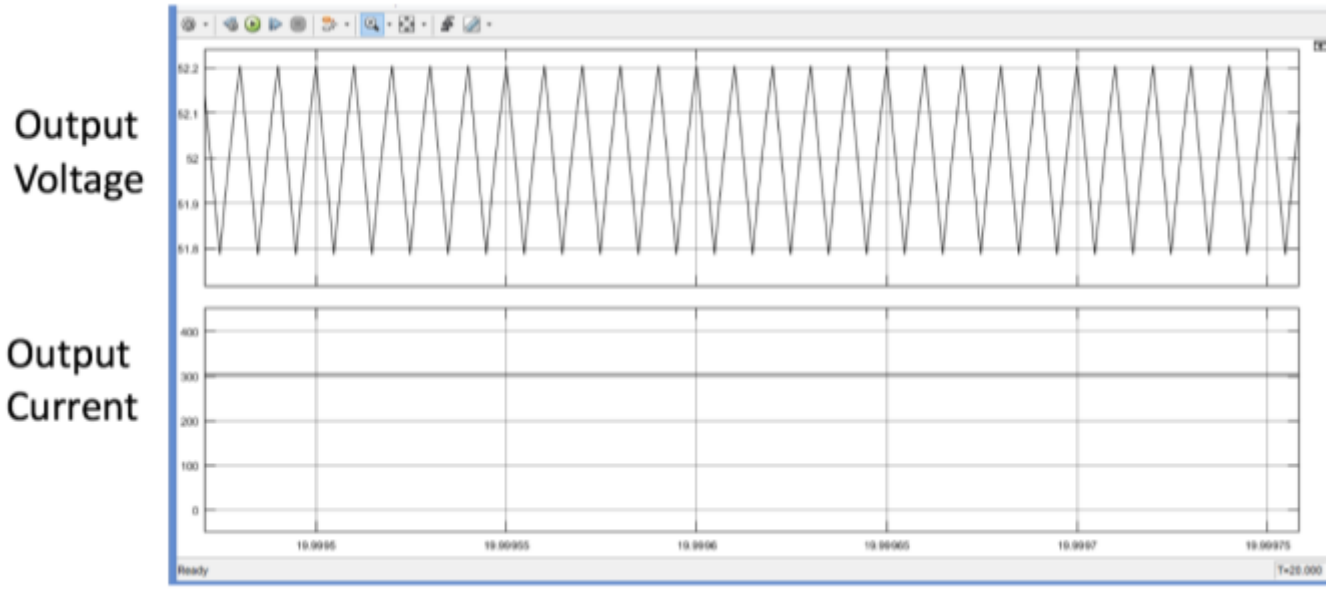

Fig. F2: Simulink simulation output voltage and current

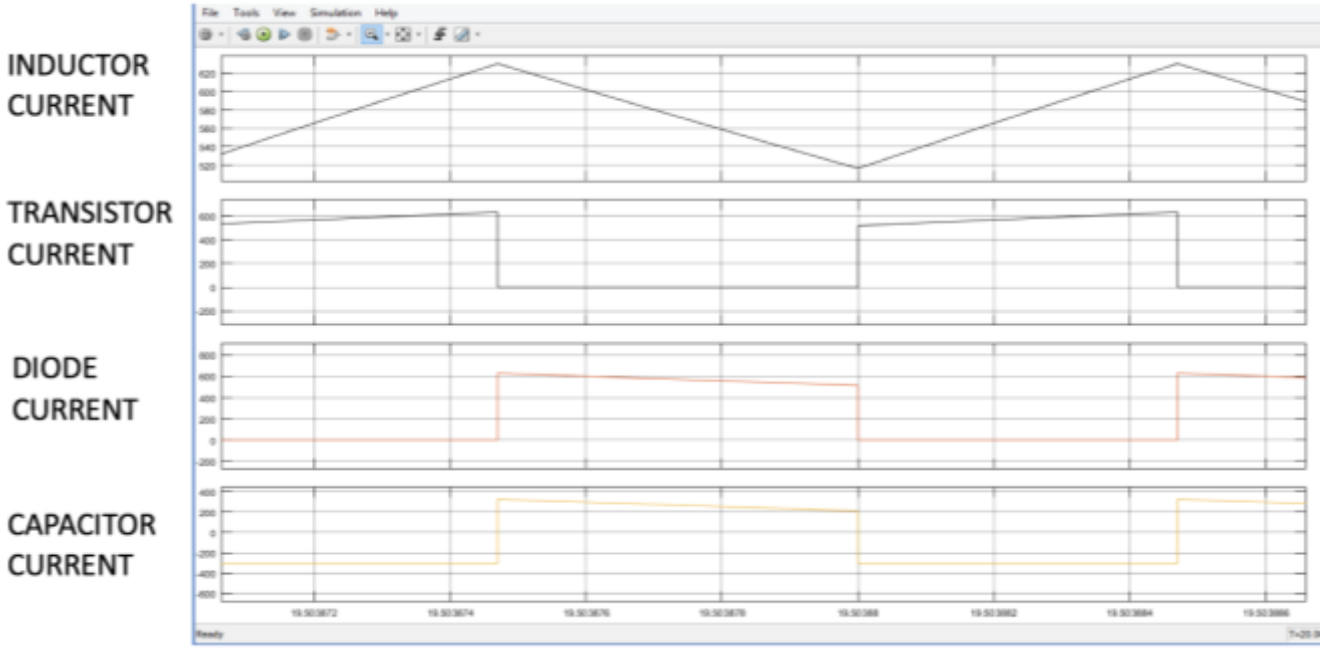

Fig. F3: Simulink simulation components currents

III. Heat Sinks and Thermal Management

Heat is one of the problems that kills or damages circuitry. It does not matter the application of the circuit, it can be for High Power Density Applications, antennas or to give

energy to a group of LEDs. Heat is an important aspect and every circuit designer should take in consideration for every design.

In the current design, thermal dissipation management was approached starting from the switchers or MOSFET for the converter, mainly because is one of the most important components and it absolutely needs the heat dissipation. Other components are the inductor and the diode. We are attacking this problem by:

- Using heat sinks.
- Adding fans.

Thermal dissipation has a general formula shown below that take into account different temperatures between two different points and depends on thermal power and thermal resistance.

$R_{\emptyset} = \frac{T1-T2}{P}$, where $R_{\emptyset} = thermal\ resistance, T1 - T2 = temparature\ difference$ and

P = thermal power [W].

This is a visual representation of the formula explain above. The P it can be interpret as the current of the circuit, and T1, T2 can be interpret as different voltages.

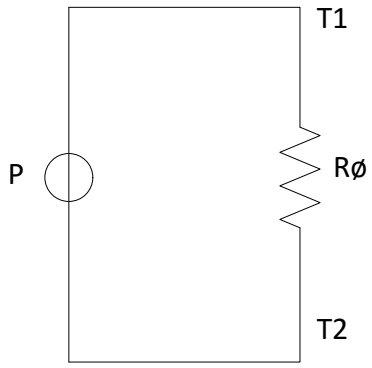

Fig. F4: Simple Thermal Circuit Diagram

MOSFETs do not have an internal junction, but the internal temperature is referred to as the junction. This junction temperature is determined by the thermal power and junction to ambient thermal resistance $R_{\emptyset}, JA$.

The manufacturer's components list, specifically show the MOSFET with a junction to ambient thermal resistance $R_{\emptyset}, JA$ as 62°C/W and a maximum junction temperature of 175°C but, designer prefer not to exceed 150°C to increase readability.

If the calculations are correct and as a result the temperature obtained with the previous equation of $R_{\emptyset}$ gave a number over the 150°C, then a heat sink is needed. The heat sink helps in the dissipation of the heat by adding more area to the element that need the dissipation of the heat.

The following formulas are used to calculate the heat dissipation of the element with the heat sink attached.

$T_s = PR_{\emptyset,SA} + T_A$; Temperature of the heat sink at near mounting point

$T_C = PR_{\emptyset,CS} + T_S = P(R_{\emptyset,CS} + R_{\emptyset,SA}) + T_A$; Temperature at device case or embodiment

$T_j = PR_{\emptyset,JS} + T_C = P(R_{\emptyset,JS} + R_{\emptyset,CS} + R_{\emptyset,SA}) + T_A$; Temperature at device junction

T_A ; this represent the ambient temperature

$R_{\emptyset,SA}$; this represent the thermal resistance between ambient temperature and heat sink

$R_{\emptyset,CS}$; this represent the thermal resistance between the case and the heat sink

$R_{\emptyset,JS}$; this represent the thermal resistance between the junction and the heat sink

The following figure is a circuit representation of the thermal dissipation with a heat sink.

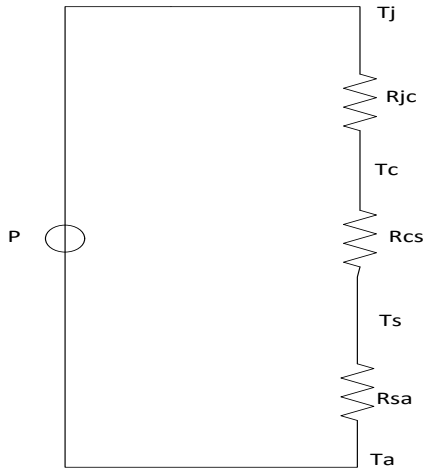

Fig. F5: Complex Thermal Circuit Diagram

The formulas discussed are going to be applied to the system and will continue to be applied in the future of this project with more in depth research in the thermal dissipation of the system.

- Thermal dissipation for the transistor implemented in the DC-DC BOOST Converter for the solar boat.

$T_j = 150°\text{C}$; $R_{CS} = .15°\text{C/W}$

$T_C = 25°\text{C}$; $R_{JS} = .12°\text{C/W}$

$T_A = 40°\text{C}$

$R_{SA} = 7.2°\text{C/W}$

Total watts (W) dissipated on one MOSFET;

$$R_{\emptyset} = \frac{T1 - T2}{Pt} = \frac{Tj - Ta}{Pt} = \frac{150 - 40}{Pt} =>$$

$$Pt = \frac{150 - 40}{R_{JC} + R_{CS} + R_{SA}} = \frac{150 - 40}{.12 + .15 + 7.2} = 14.73W$$

Total temperature that one MOSFET will be subjective at;

$$T_j = 14.73(.12 + .15 + 7.2) + 40 = 150.0331°C$$

This will be for each MOSFET. The implementation of the boost converter will have two (2) MOSFET in parallel to divide the current between the two.

- Thermal dissipation for the diode implemented in the DC-DC BOOST Converter for the solar boat.

VS-100BGQ100 MODEL

$T_j = 150°C \ ; R_{CS} = .30°C/W$

$T_C = 25°C \ ; R_{JS} = .50°C/W$

$T_A = 40°C$

$R_{SA} = 7.2°C/W$

Total watts (W) dissipated on one MOSFET;

$$R_{\emptyset} = \frac{T1 - T2}{Pt} = \frac{Tj - Ta}{Pt} = \frac{175 - 40}{Pt} =>$$

$$Pt = \frac{175 - 40}{R_{JC} + R_{CS} + R_{SA}} = \frac{175 - 40}{.50 + .30 + 7.2} = 16.875W$$

Total temperature that one MOSFET will be subjective at;

$$T_j = 16.875(.50 + .30 + 7.2) + 40 = 175.003°C$$

This will be for each diode. The implementation of the boost converter will have ten (10) diodes in parallel to divide the current.

Using Heatsink Calculator program the team can simulate the size of the heatsink necessary to dissipate the heat created by the elements of the circuits.

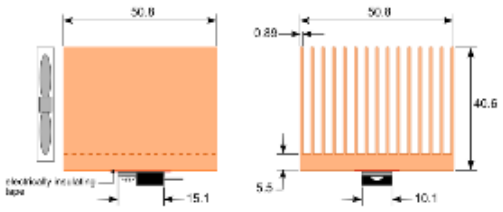

Fig. F6: Thermal Analysis Program

The first step in the program let the user create the heat sink if the user desire or the program let you select some in the tables included in the same program.

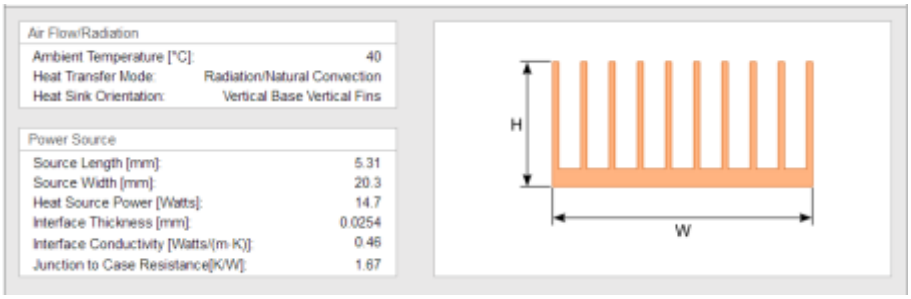

Fig. F7: Heatsink Data Base

Once the heatsink is selected, the area of use for the element touching the heatsink is selected. The number of inputs are the width, length, power dissipated by the element, thermal interface (thermal paste) and the resistance junction-case.

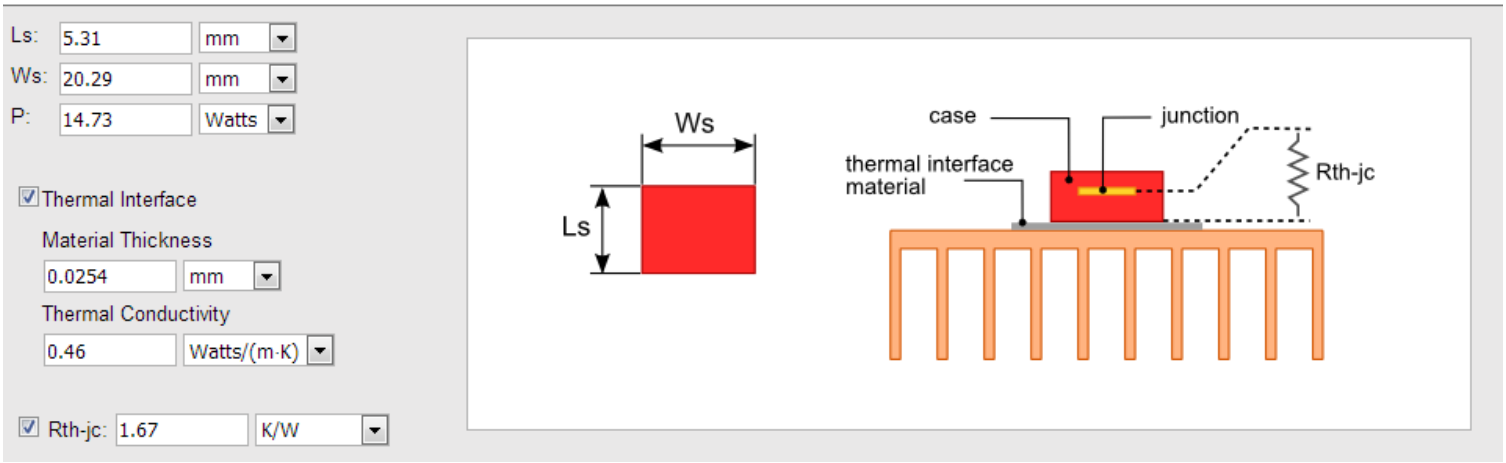

Fig. F8: Area of the element in the heatsink

Next, the user inputs the ambient temperature and the air convention selecting from natural convention (best known as passive convention) or active cooling which includes a fan.

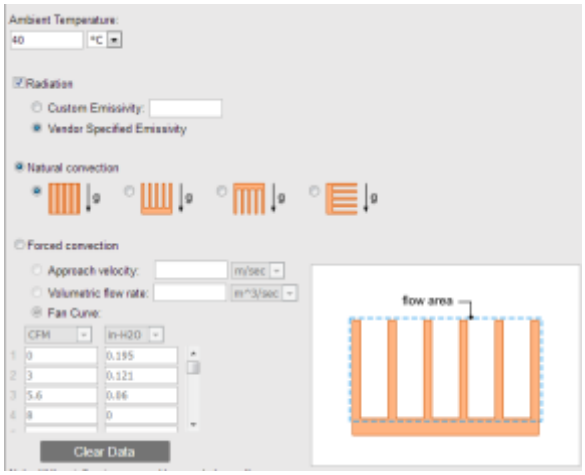

Fig. F9: Airflow convention

The heatsink for the boost converter is 12 in by 12 in by 1 in for and it maintain the temperature of the elements under 150˚C this is shown in fig. F10.

Thermal Parameters	
Ambient Temperature [°C]:	40
Source Temperature [°C]:	120
Temperature Difference [°C]:	79.8
Heat Sink Thermal Resistance [K/W]:	1.39

Fig. F10: Results for boost converter heatsink

Appendix G: Drive Train Design

In order to analyze the shaft, a shaft analysis was executed. The shaft is on a vertical position, this implies and the shaft does not produce a significant moment through the shaft. With this on mind, the bending stress depends on the momentum and this implies that the bending stress is 0. Because there is no external force apart from the torsion, shear stress should not be observed. The only force affecting the shaft is the torque transmitted by the motor. The only stress that we have affecting on our shaft is torsional stress. To calculate the torque transmitted by the motor, the team made an instrument to measure the motor's angular velocity, power, thrust, and boat speed. The following figure shows the behavior of the boat. The shaft has 3 cross-sectional areas with dimeters of 0.625in (16.51mm), 0.60in (15.24mm), and 0.75in (19.05mm). The analysis was made on the cross sectional area (0.65in) because on this area is located a keyway to transmit the torque of the motor. This keyway creates a stress concentration factor that represented the weakest area on the shaft.

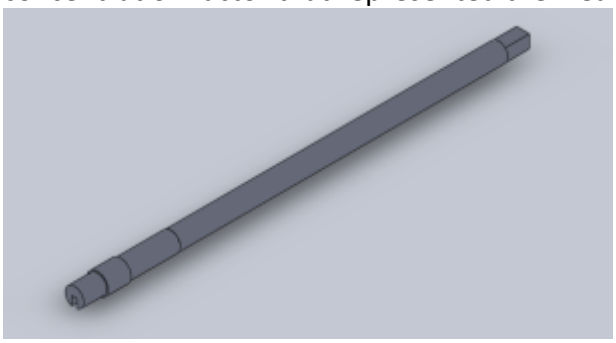

Figure 3 New stainless steel shaft 3d cad.

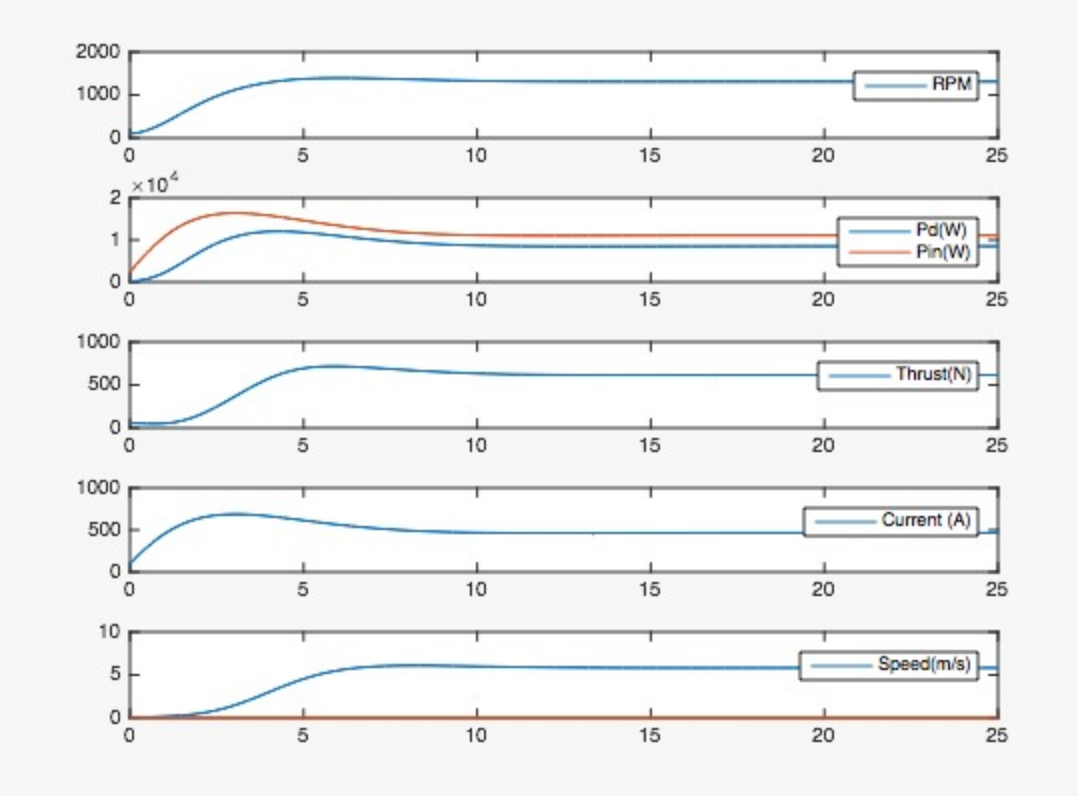

Fig. G1: Last year's lecture of power, speed, thrust and RPM

D=0.65in=16.51mm=0.01651m

I. Static analysis:

Maximum Torque:

$$T(N-M)=\frac{Power(Watts)}{\omega(RPM)}=\frac{8{,}000W}{1300rpm}*\frac{60sec}{2\Pi}=58.76\text{N-m}$$

$$J=\frac{\pi}{32}d^4=\frac{\pi}{32}0.01651m^4=7.2943X10^{-9}$$

$$\tau_{torsion}=\left(K*\frac{\left(\frac{Td}{2}\right)}{\frac{\pi}{32}d^4}\right)=\frac{\left(\frac{58.76n-m)(0.01651m)}{2}\right)}{\frac{\pi}{32}*(0.01651m)^4}=k*66.49MPa$$

The K is the stress concentration factor that creates the keyway on the shaft. This K is equal to 1.6.

$$\tau_{torsion}=\left(K*\frac{\left(\frac{Td}{2}\right)}{\frac{\pi}{32}d^4}\right)=1.6\frac{\left(\frac{58.76n-m)(0.01651m)}{2}\right)}{\frac{\pi}{32}*(0.01651m)^4}=106.38MPa$$

To compare the torsion on the other cross sectional area.

D= 0.60in= 15.24mm

$$\tau_{torsion} = \left(K * \frac{\left(\frac{Td}{2}\right)}{\frac{\pi}{32}d^4} \right) = 1 \frac{\left(\frac{58.76n-m)(0.01524m)}{2}\right)}{\frac{\pi}{32}*(0.01524m)^4} = 84.54MPa$$

On this area the shaft not have a stress concentration factor and this implies K=1.

D=0.75in=19.05in

$$\tau_{torsion} = \left(K * \frac{\left(\frac{Td}{2}\right)}{\frac{\pi}{32}d^4} \right) = 1 \frac{\left(\frac{58.76n-m)(0.01905m)}{2}\right)}{\frac{\pi}{32}*(0.01905m)^4} = 43.28MPa$$

On this area the shaft not have a stress concentration factor and this implies K=1.

For the analysis we took the weakness point on the shaft that is on the cross sectional area of Diameter=0.65.

Von Mises stress= the total stress on the shaft

$$\sigma_{VM} = \sqrt{(\sigma_1)^2 + (\sigma_2)^2 - (\sigma_1)^2(\sigma_2)^2 + 3\left(\tau_{xy}\right)^2}$$

On this area the shaft does not have a stress concentration factor and this implies K=1.

The Representation, the bending, and axial stress on the shaft and the representation the sum of torsional and shear stress. Previously, we demonstrated that the shaft does not have any stress on bending, shear and axial with this on mind the only stress on the equation is the torsion stress.

$$\sigma_{VM} = \sqrt{\left(\sigma_{bending}\right)^2 + 3(\tau_{torsion})^2}$$

$$\sigma_{VM} = \sqrt{(0)^2 + 3(106.38)^2} = 184.25 \text{ Mpa}$$

$\sigma_{yield} = 206\text{Mpa or } 30\text{Ksi}$ this is a material properties.

$$\frac{\sigma_{yield}}{SF} = \sqrt{\left(\frac{\sigma_{bending}}{}\right)^2 + 3\left(\frac{\tau_{torsion}}{}\right)^2} = \sqrt{(0)^2 + 3(106.38)^2} = 1.11$$

II. Dynamic analysis.

The dynamic test depends on a mean and amplitude stress. For this analysis, we used the Modified Goodman theory.

$$\text{Modified-Goodman:} \quad n_f = \frac{1}{\frac{\sigma_a}{S_e} + \frac{\sigma_m}{S_{ut}}}$$

Fig. G2: Modified-Goodman equation

On torsional stress only exist a $\tau_{torsion}\ mean$ and the $\tau_{torsion}\ amplitud$ = 0.

This simplified the equation to $Sf = \frac{Sut}{\sigma m}$ no matter what was calculated the Se = Se corrected to obtain parameters of the ultimate tensile stress with correction factor for the selected material. Is the ultimate tensile strength that is a material property.

$S_{UT} = 75ksi\ or\ 515Mpa$

$S_{e\ uncorrected} = 0.5 * S_{UT} = 0.5 * (75ksi) = 37.5ksi$

$S_{e\ corrected} = 0.5 * S_{UT} * kload * ktemp * kreliability * ksize * ksurface = 0.5 * (75ksi)$

Factors for dynamic test (surface, reliability, temperature, size and load)

K_{surf}

$K_{surf}(cold\ rolled) = a * Sut^{.b}$

Table G3: Surface Factor Parameters Table

	MPa		kpsi	
Surface Finish	A	b	A	b
Ground	1.58	−0.085	1.34	−0.085
Machined or cold-rolled	4.51	−0.265	2.7	−0.265
Hot-rolled	57.7	−0.718	14.4	−0.718
As-forged	272	−0.995	39.9	−0.995

$K_{surf}(cold\ rolled) = 2.7 * 75^{-0.265} = 0.859$

K_{load}

> NOTE: If one uses von Mises effective stresses, thus adjusting for shear vs. normal stresses K_{load} for torsion is *1*.

$K_{load} = 1$

K_{temp}

$K_{temp} = St/Srt$

We have a ambient temperature that is around 20 Celsius when we look to the table $K_{temp} = 1$

Table G4: Temperature Factor Parameters Table

Temperature, °C	S_T/S_{RT}	Temperature, °F	S_T/S_{RT}
20	1.000	70	1.000
50	1.010	100	1.008
100	1.020	200	1.020
150	1.025	300	1.024
200	1.020	400	1.018
250	1.000	500	0.995
300	0.975	600	0.963
350	0.943	700	0.927
400	0.900	800	0.872
450	0.843	900	0.797
500	0.768	1000	0.698
550	0.672	1100	0.567
600	0.549		

K_{reliab}

We decide that we want a reliability % = 99

Reliability, %	Transformation Variate z_a	Reliability Factor k_e
50	0	1.000
90	1.288	0.897
95	1.645	0.868
99	2.326	0.814
99.9	3.091	0.753
99.99	3.719	0.702
99.999	4.265	0.659
99.9999	4.753	0.620

Figure 8 Reliability factor parameters

$K_{reliab}(99\%) = 0.814$

.

$$for\_d \le 0.3in\_(8mm):.....k_{size} = 1$$
$$for\_0.3in \le d \le 10.in:.....k_{size} = 0.869 d_{equivalent}^{-0.097}$$
$$for\_8mm \le d \le 250mm:.....k_{size} = 1.189 d_{equivalent}^{-0.097}$$

$K_{size} = 0.869 * d_{eq}^{-0.097} = 0.906$ $\quad\quad$ $d_{eq}(Rotating) = \sqrt{\frac{A_{95}}{0.0766}}$

$A_{95} = 0.0766 d_{eq}^2$

$\boldsymbol{\sigma_{corrected}}: 0.5(75ksi)(0.859)(0.814)(1)(1)(0.906) = 23.75ksi=$

For dynamic

$\sigma_{amplitude} = 0\ with\ \sigma_{mean} = 184\ Mpa$:

$\tau_{torque,mean} = K_{torque}\left[\frac{Tc}{J}\right] = \frac{K_{torque}T\left(\frac{d}{2}\right)}{\frac{\pi}{32}d^4} = 106$ Mpa

$\tau_{torque,amp}$

$\sigma_{Mean} = \sqrt{\left(\sigma_{bending\ mean}\right)^2 + 3(\tau_{torsion\ mean})^2} = \sqrt{(0)^2 + 3\left((106)Mpa\right)^2} = 184$ Mpa

$\sigma_{Amplitued} = \sqrt{\left(\sigma_{bending\ amp}\right)^2 + 3\left(\tau_{torsion\ amp}\right)^2} = \sqrt{(0)^2 + 3(0)^2} = 0$ Mpa

$$\frac{\sigma_{amp}}{Se_{,corrected}} + \frac{\sigma_{mean}}{Sut} = \frac{1}{SF}$$

$$\frac{0Mpa}{163.75Mpa} + \frac{184Mpa}{515Mpa} = \frac{1}{SF} \qquad Sf=2.85$$

MJSC41-16-A, 16mm Jaw Coupling Hub, Aluminum

Quantity Break	Price in USD
1	$36.69
10	$34.01
25	$28.35
50	$25.51
100	Request Quote

Availability: In Production
Typical Lead Time: 0-2 Days
Request a Lead Time

1 Add to Cart

BETTER PRICING MAY BE AVAILABLE THROUGH YOUR LOCAL DISTRIBUTOR

Product Number:	MJSC41-16-A
Product Type:	Jaw Coupling Hub
Style:	Set Screw with Keyway
Material:	2024 or 7075 Aluminum
Finish:	Bright
Manufacturer:	Ruland Manufacturing
UPC Number	634529116449
Country of Origin:	USA

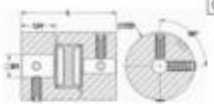

Choose a CAD format

Download CAD File

Installation Instructions

Dimensions

Bore B1:	16 mm
Keyway K1:	5 mm
Outer Diameter OD:	41.3 mm
Length L:	93.0 mm
Hub Length LH:	18.0 mm
B1 Max Shaft Penetration:	18.0 mm

Fastening Hardware

Forged Set Screw:	M5
Number of Screws:	2 ea 90° apart
Screw Material:	Alloy Steel
Screw Finish:	Black Oxide
Seating Torque:	4 Nm
Hex Wrench:	2.5 mm

Assembles with

Hubs:	MJC41, MJS41, MJCC41, JC26, JS26, JCC26, JSC26
Coupling Insert:	JC26/41-98A JC26/41-92A

Torque Specifications

Ratings vary with coupling insert select

Misalignment

Ratings vary with coupling insert select

Additional Information

Maximum Speed:	8,000 RPM
Bore Tolerance:	+.03 mm / +.00 mm
Weight:	0.163 lbs
Temperature Range:	-10°F to 180°F -23°C to 82°C

Certifications/ Standards

ISO 9001: 2008	Certified
Conflict Minerals	Compliant
RoHS2:	Compliant
REACH:	Compliant

Product Notes

Note 1: Stainless steel hubs are available upon request.

Note 2: Performance ratings are for guidance only. The user must determine suitability for a particular application.

JD26/41-92Y, Jaw Coupling Spider, 92 Shore A Yellow

Quantity Break	Price in USD
1	$18.98
10	$11.39
25	$9.48
50	$8.54
100	Request Quote

Availability: In Stock

1 Add to Cart

BETTER PRICING MAY BE AVAILABLE THROUGH YOUR LOCAL DISTRIBUTOR

Product Number:	JD26/41-92Y
Product Type:	Jaw Coupling Spider
Style:	Spider Insert
Material:	Polyurethane 92 Shore A YELLOW
Manufacturer:	Ruland Manufacturing
UPC Number	634529068977
Country of Origin:	USA

Choose a CAD format

Download CAD File

Installation Instructions

Dimensions

Outer Diameter OD:	1.625 in / 41.3 mm

Assembles with

Hubs:	JC26, JS26, JCC26, JSC26, MJC41, MJS41, MJCC41, MJSC41
Coupling Insert:	JD26/41-98A

Torque Specifications

Nominal Torque:	97 in-lb, 11.0 Nm
Peak Torque:	194 in-lb, 22.0 Nm

Misalignment

Angular Misalignment:	0.9°
Parallel Misalignment:	0.006 in, 0.15 mm
Axial Motion:	0.05 in, 1.27 mm

Additional Information

Torsional Stiffness:	0.012 Deg/in-lb, 0.106 Deg/Nm
Maximum Speed:	8,000 RPM
Weight:	0.025 lbs
Temperature Range:	-10°F to 180°F -23°C to 82°C

Certifications/ Standards

ISO 9001: 2008	Certified
Conflict Minerals	Compliant
RoHS2:	Compliant
REACH:	Compliant

Tight-Tolerance Highly Corrosion-Resistant 316 Stainless Steel Rods

- Yield Strength: 30,000 psi
- Hardness: Rockwell B75 (Medium)
- Temper Rating: Softened
- Heat Treatable: No
- Specifications Met: ASTM A276, AMS 5648

The diameter of these precision-ground rods is held to a ±0.0005" tolerance. Made of 316/316L stainless steel, they contain less carbon than standard 316 for better weldability. The addition of molybdenum gives this material excellent corrosion resistance. Use it in a variety of marine and chemical-processing applications. This material maintains its corrosion resistance in temperatures up to 1500° F.

Dia.	Dia. Tolerance	Fabrication	Straightness Tolerance		1/2 ft. Lg.	1 ft. Lg.	2 ft. Lg.	3 ft. Lg.	6 ft. Lg.
1/8"	-0.0005" to 0.0005"	Heat Treated	1/8" per 6 ft.	8936K1	$3.49	$5.37	$9.50	$12.39	$20.65
3/16"	-0.0005" to 0.0005"	Heat Treated	1/8" per 6 ft.	8936K2	3.94	6.07	10.74	14.00	23.34
1/4"	-0.0005" to 0.0005"	Heat Treated	1/8" per 6 ft.	8936K3	4.43	6.81	12.05	15.71	26.19
5/16"	-0.0005" to 0.0005"	Heat Treated	1/8" per 6 ft.	8936K4	5.29	8.14	14.40	18.79	31.31
3/8"	-0.0005" to 0.0005"	Heat Treated	1/8" per 6 ft.	8936K5	6.89	10.60	18.75	24.46	40.77
7/16"	-0.0005" to 0.0005"	Heat Treated	1/8" per 6 ft.	8936K24	9.14	14.06	24.87	32.44	54.07
1/2"	-0.0005" to 0.0005"	Heat Treated	1/8" per 6 ft.	8936K6	10.51	16.17	28.60	37.31	62.18
9/16"	-0.0005" to 0.0005"	Heat Treated	1/8" per 6 ft.	8936K25	13.64	20.99	37.14	48.44	80.73